UNIVERSIDADE FEDERAL DE ALAGOAS

INSTITUTO DE QUÍMICA E BIOTECNOLOGIA

PROGRAMA DE PÓS-GRADUAÇÃO EM QUÍMICA E BIOTECNOLOGIA

ANNA CAROLINE LIMA CANDIDO

DEVELOPMENT OF ELECTROCHEMICAL HISTAMINE BIOSENSOR FOR HISTAMINE USING GENETICALLY ENGINEERED HISTAMINE DEHYDROGENASE FROM *RHIZOBIUM SP* WITH GOLD-BINDING PEPTIDE TAG

MACEIÓ - AL

2021

ANNA CAROLINE LIMA CANDIDO

DEVELOPMENT OF ELECTROCHEMICAL HISTAMINE BIOSENSOR FOR HISTAMINE USING GENETICALLY ENGINEERED HISTAMINE DEHYDROGENASE *RHIZOBIUM SP* WITH GOLD-BINDING PEPTIDE TAG

Thesis submitted to the graduate degree program in Chemistry in Biotechnology of the Federal University of Alagoas in fulfillment of the requirements for the degree of Doctor in Sciences.

Advisor: Profª. Drª. Fabiane Caxico de Abreu Galdino

Co-advisor: Dr Mark Richter (*in memorian*) – Kansas University

MACEIÓ - AL

2021

FOLHA DE APROVAÇÃO

Membros da Comissão Julgadora da Defesa de Tese da Doutoranda **Anna Caroline Lima Candido** intitulada: **"Desenvolvimento de Biossensor Eletroquímico para Histamina Utilizando Histamina Desidrogenase Rhizobium Sp geneticamente modificada com Peptídeo de Afinidade ao Ouro",** apresentada ao Programa de Pós-Graduação em Química e Biotecnologia da Universidade Federal de Alagoas no dia 23 de agosto de 2021, às 14 h, por meio de videoconferência.

Comissão Examinadora:

Profa. Dra. Fabiane Caxico de Abreu Galdino

Orientadora (PPGQB/IQB/UFAL)

Prof. Dr. Diógenes Meneses dos Santos

(PPGQB/IQB/UFAL)

Profa. Dra. Anielle Christine Almeida Silva

(IF/UFAL)

Profa. Dra. Sônia Salgueiro Machado

(IQB/UFAL)

Painho e Mainha ♥

(Seu Artur e Dona Rosinha).

AGRADECIMENTO

"Em tudo dai graças, porque esta é a vontade de Deus em Cristo Jesus para convosco" (1 Tessalonicenses 5:18). Como em tudo na minha vida, agradeço à Deus por todas as oportunidades e pela família que tenho.

Painho e Mainha, meu eterno agradecimento, nenhuma das minhas conquistas seriam possíveis sem o incentivo e apoio que recebi de vocês a vida inteira.

Isse e Clara, minhas irmãs ou sis, como dizemos, obrigada por me entenderem, diante de toda complexidade que carrego dentro de mim, vocês conseguem me compreender melhor que ninguém, por tantos anos dividimos o mesmo lugar e tantas vezes vocês permitiram que nosso quarto fosse só meu e por isso puder estudar um pouco melhor e concluir tantas etapas da minha vida.

À minha família maravilhosa (tias, tios, primas, primos e avós), meus exemplos, maiores incentivadores, e aqueles que sempre acreditam mais em mim do que eu mesma. Obrigada por tudo e por tanto.

Aos amigos que a UFAL me deu, em especial Marílya, Bia, Val e Amanda que nossos momentos juntos estão guardados em um cantinho muito especial das minhas memórias.

Aos meus amigos de Laboratório e de vida, Samaysa, Marílya, Renata e Ygor, uma das minhas maiores saudades é a hora do café com vocês, sempre regado de muitas conversas e risadas. Que sorte eu tive de ter vocês comigo nessa jornada.

Ao LEMAN que foi minha casa na UFAL durante tantos anos e que sempre foi um ponto de encontro para tantos alunos.

A minha querida orientadora, Prof. Dra Fabiane Caxico, que está comigo a tantos anos, que sempre foi muito paciente, que me ensinou, me deu bronca e me apoiou em todos os momentos, especialmente quando decidi fazer doutorado sanduíche no exterior, serei eternamente grata por tudo.

Ao Professor Dr. Diógenes que foi essencial durante meu doutorado, através dele conheci do trabalho do Prof. Dr. Mark, e foi a ponte para que eu pudesse ir aos Estados Unidos e realizar esse trabalho. Muito Obrigada.

Ao meu segundo orientador o Dr. Mark Richter, que nos deixou tão cedo, junto com tantos outros durante a pandemia, mas que além do comprometimento com a ciência e a vontade de fazer algo diferente, ele, junto com sua esposa Kim, me ensinou

tanto sobre gentileza e bondade. Agradeço também a todos do Richter's Lab, em especial a Priyanka, que me guiou desde o primeiro dia no laboratório e Dr. George Wilson por sua generosidade ao transmitir seu vasto conhecimento e sempre nos dar verdadeiras aulas em simples reuniões.

Ao meu marido, que chegou no meio de tudo isso, mesmo sem entender, deu todo suporte e foi fundamental para eu manter a sanidade quando tudo parecia não tem mais sentido

Aos membros da banca avaliadora pela disponibilidade e o aceite do convite em avaliar este trabalho, que marca uma etapa tão importante da minha carreira acadêmica e profissional.

A Universidade Federal de Alagoas, que é como minha segunda casa e onde encontrei amigos para a vida toda.

À Universidade de Kansas pela recepção tão acolhedora.

Ao Programa de Doutorado Sanduíche no Exterior e a CAPES pela bolsa fornecida.

Ao Programa de Pós-Graduação em Química e Biotecnologia da UFAL.

RESUMO

A histamina é uma amina biogênica essencial que atua como um neurotransmissor e foi descoberto que desempenha um papel fundamental em muitas doenças neurológicas e psiquiátricas. Sendo assim, existe uma demanda considerável pela determinação da histamina para análises do tipo *point-of-care*, visando ao diagnóstico e prevenção de doenças. Para tanto, avaliamos um par redox, de alto *turnover* (K_{cat}), envolvendo a enzima histamina desidrogenase de Rhizobium sp. 4-9 (HDR), que contém um mononucleotídeo de flavina ligado covalentemente e um centro de ferro-enxofre que transfere elétrons entre a flavina reduzida e os receptor externo de elétrons. Existe um interesse significativo na imobilização desta enzima para melhorar a estabilidade catalítica em superfícies condutoras em relação a aplicações de biossensor. Neste trabalho a enzima HDR foi geneticamente projetada para ter um peptídeo com alta afinidade ao ouro (cAuBP), no C ou N-terminal, para imobilização seletiva da enzima em superfícies de ouro e avaliar a atividade catalítica das proteínas após a fusão. A eficiência da transferência de elétrons de enzimas redox pode ser difícil na ausência de mediador, portanto o 1,1-ferrocenodimetanol foi escolhido para realizar todos os experimentos, porém na sua forma oxidada. A enzima exibe alta seletividade a histamina e sem inibição por substrato, mesmo com alto *turnover* (K_{cat} aparente> 127s-1) observadas usando um ferroceno solúvel, diferentemente da histamina desidrogenase de *Nocardioides simplex*. Experimentos de voltametria cíclica (CV) e amperometria foram realizados usando um sistema de três eletrodos com uma célula eletroquímica convencional equipada com Ag/AgCl como eletrodo de referência, um eletrodo de platina como contra-eletrodo e um eletrodo de disco de ouro, como eletrodo de trabalho. A possibilidade de transferência direta de elétrons (DET) entre a enzima e o eletrodo também foi avaliada e assim como mediada pelo derivado do ferroceno. Voltamogramas cíclicos e amperometria do ferroceno oxidado e HDR de Rhizobium sp. 4-9 foram registrados na presença e ausência de histamina, em tampão fosfato pH 7,4. Altas taxas de transferência de elétrons entre a histamina e um eletrodo de ouro foram observadas quando o ferroceno oxidado está em solução. Microscopia de força atômica (AFM) e ressonância plasmática de superfície (SPR) e localizada (LSPR) foram realizadas para avaliar a afinidade de ligação às superfícies de ouro. A especificidade, propriedades cinéticas, falta de inibição por substrato e estudos eletroquímicos indicam que HDR é adequada para uso em aplicações como biossensor.

Palavra-chave: Biossensor, histamina, peptídeos, ouro.

ABSTRACT

Histamine is an essential biogenic amine that acts as a neurotransmitter and has been found to play a key role in many neurological and psychiatric diseases. Thus, there exists a considerable demand for determining histamine for point-of-care analysis aimed to disease diagnosis and prevention. To this end, we have evaluated a high-turnover redox couple involving the enzyme histamine dehydrogenase from *Rhizobium sp.* 4-9 (HDR) which contains a covalently attached flavin mononucleotide and an iron-sulfur center that shuttles electrons between the reduced flavin and external electron acceptors. There is a significant interest in the immobilization of this enzyme to improve catalytic stability on conductive surfaces towards biosensing applications. Here we engineered HDR construct with a functional cyclic gold-binding peptide (cAuBP) tag, at the C and N terminus, to immobilize the enzyme onto gold surfaces and evaluate the catalytic activity of fusion proteins. The electron transfer efficiency of redox enzymes can be difficult in the absence of mediator, thus 1,1-ferrocenedimethanol was chosen to perform all the experiments, on its oxidized form. The enzyme exhibits high substrate selectivity without substrate inhibition even at high turnover rates (apparent $K_{cat} > 127 s^{-1}$) observed using soluble ferricenium substrates, unlike the closely related histamine dehydrogenase from *Nocardioides simplex* (*ns*HDR). Cyclic voltammetry (CV) and Amperometry experiments were carried out using a three electrodes system with a conventional cell equipped with an Ag/ AgCl electrode as the reference electrode, a platinum electrode as the counter electrode, and gold disc electrode as the working electrode. The possibility of Direct Electron Transfer (DET) between the enzyme and electrode was evaluated and mediated by the ferrocene derivative as well. Cyclic voltammograms and Amperometry of oxidized ferrocene and HDR from *Rhizobium sp.* 4-9 were recorded in the presence and absence of histamine, in Phosphate Buffer pH 7.4. High rates of electron transfer between histamine and a gold electrode were observed when the oxidized ferrocene is in solution. Atomic force microscopy, Localized Surface Plasmon Resonance (LSPR) and Surface Plasmon Resonance (SPR) were performed to evaluate the binding affinity to gold surfaces. The specificity, kinetic properties, lack of substrate inhibition and electrochemical studies indicate the suitability of the HDR for use in biosensing applications.

LIST OF FIGURES

LIST OF TABLES

TABLE OF ABBREVIATIONS

Au	Gold
E	Potential
I	Current
mV/s	Millivolts Per Second
pH	Potential of Hydrogen
CV	Cyclic Voltammetry
µA	Microampère
ν	Scan Rate
HDR	Histamine Dehydrogenase from *Rhizobium Sp.*
nsHDR	Histamine Dehydrogenase from *Nocardioides Simplex*
DET	Direct Electron Transfer
LSPR	Localized Surface Plasmon Resonance
SPR	Surface Plasmon Resonance
CNS	Central Nervous System
FMN	Flavin Mononucleotide
FAD	Flavin Adenine Dinucleotide
SAM	Self-Assembled Monolayers
ET	Electron Transfer
GBP	Gold-Binding Peptides
AuNP	Gold Nanoparticle
cAuBP	Cyclic Gold Binding Pep
PCR	Polymerase Chain Reaction

IPTG	Isopropyl B-D-1-Thiogalactopyranoside
SDS PAGE	Sodium Dodecyl Sulfate Polyacrylamide Gel Electrophoresis
FCDM⁺	Ferriciniumdimethanol
SEC	Size Exclusion Chromatography
RDE	Rotating Disk Electrode
K$_{cat}$	Catalytic Constant/ Turnover Number
K$_m$	The Michaelis Constant
ATM	Atomic Force Microscopy
TSG	Template Stripped Gold
ε	Extinction Coefficient
TEV	Cysteine Protease from Tobacco Etch Virus

TABLE OF CONTENTS

1 INTRODUCTION

Histamine is an essential biogenic amine that acts as a neurotransmitter, mediates allergic reactions, plays a role in cell proliferation, and is important in signaling the release of gastric acid into the stomach (THURMOND; GELFAND; DUNFORD, 2008) and has been found to play a key role in many neurological and psychiatric diseases such as sleep disorders, disorders of mood and cognition (schizophrenia, depression, Alzheimer's disease), movement disorders (Parkinson's disease), epilepsy, eating disorders, pain, neuroinflammation and addiction (HAAS; SERGEEVA; SELBACH, 2008).

The ability to simultaneously measure changes in histamine concentration within specific brain structures in conjunction with other physiological changes is essential to understanding the physiological role of histamine in these disorders. To date, histamine detection in the central nervous system has been accomplished using microdialysis techniques (FLIK et al, 2015) and associated off-line analysis techniques such as high-performance liquid chromatography (KEHR; YOSHITAKE, 2013). Our goal is the development of a biosensor specific for histamine that needs to be suitable for in vivo implantation and recording. Applying biosensor technologies to the *in vivo* measurement of histamine may prove to be a useable platform for monitoring changes in brain histamine concentration. Second-by-second histamine biosensor readings can then be paired with biosensors specific for other analytes such as glutamate, lactate or glucose.

The *in vivo* electrochemical monitoring of neurotransmitters in the brain have been effective for electroactive species (e.g., dopamine, norepinephrine, serotonin, adenosine, etc.). However, several challenges remain to be solved: (1) many chemical species in the brain have similar oxidation/reduction potentials and the presence of many interfering species makes it difficult to conduct multi-analyte detection *in vivo*. (2) non-electroactive species, such histamine requires enzymes to be detected electrochemically. Hence, a sensing technique that is reliable and allows simultaneous real-time multi-analyte detection with high specificity, temporal and spatial resolution is greatly needed (SI; SONG, 2018)

Biosensors are a simple, robust and economical analytical devices based on the principle of the interaction of biological elements to a certain analyte and the generation of physicochemical changes, such as transfer of electrons. Amongst the

presently available biosensor systems, electrochemical biosensors hold leading positions for their high performance, simple design, rapid screening methods, low cost, low detection limits and the possibility of miniaturization (LOPEZ; REDONDO-GOMEZ; LOPEZ-RUIZ, 2017). In particular, enzymatic amperometric biosensors have attracted enormous attention in electroanalysis during the last decade. These devices unite the enzyme selectivity for the identification of a specific target analyte with the direct transduction of the rate of the biocatalytic reaction into a current signal, enabling rapid, sensitive, and accurate detection (VERMA et al, 2020).

For histamine analysis, amperometric biosensors have been proposed using histamine dehydrogenase from *Nocardioides simplex* (*ns*HDR) (YAMADA et al 2008) but is strongly susceptible to substrate inhibition from histamine at high concentrations (TSUTSUMI et al, 2009a) and is also active toward other biological amines, for example putrescene (SIDDIQUI et al 2000). Due to its lack of substrate specificity as well and substrate inhibition this enzyme was not considered here. However, a similar histamine dehydrogenase from *Rhizobium* sp. was identified and partially characterized (BAKKE et al, 2005) that showed remarkably high specificity towards histamine with essentially no observable activity toward other biological amines. The enzyme also has catalytic properties that are suitable for use on a biosensor and is not subject to substrate inhibition (BAKKE et al, 2005; TSUTSUMI et al, 2009a).

Inorganic-binding peptide tags have emerged as alternative surface functionalization and consequently an immobilization method due to their molecular recognition, self-assembly, and ease of synthetic and genetic manipulation properties. The selective and strong binding properties of biocombinatorially selected peptides have been exploited in different applications ranging from biocompatible surface modifications, assembly of nanoscale objects, development of sensing platforms, and inorganic material synthesis (TAMELER et al, 2006; CENTINEL et al 2013; LEE et al 2018). In this work, we investigated the use of a selected and well-characterized gold-binding peptide tag (HNILOVA et al, 2008) as an immobilization approach for directed self-attachment of HDR from *Rhizobium* sp. 4-9 onto a variety of gold surfaces including nanoparticles and electrodes for a desired electrochemical biosensor application.

1.1 Histamine

Histamine was first synthesized (1907) and isolated as a bacterial contaminant of an extract of ergot (1910), the elucidation of its role in health and disease and its molecular mechanism of action have been continuous, reflecting the application of advances in scientific knowledge, technology and therapeutics over the last 100 years (THURMOND, 2010).

Histamine (2-[3H-imidazol-4-yl]ethanamine) (Figure 1)is an important chemical mediator that causes vasodilation and increased vascular permeability and may even contribute to anaphylactic reactions. It also acts on several physiological functions, such as cell differentiation, proliferation, hematopoiesis, and cell regeneration. Synthesis of histamine occurs through decarboxylation of the aminoacid histidine by the enzyme L-histidine decarboxylase, which is expressed in neurons, parietal cells, gastric mucosal cells, mast cells, and basophils; degradation of histamine is mediated by the enzyme diamine oxidase and histamine N-methyltransferase, which catalyzes histamine deamination (BRANCO et al, 2018).

Figure 1 - Chemical structure of histamine
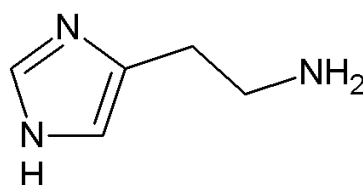
Histamine

Source: Author, 2020

Apart from its central role in the mediation of allergic reactions, gastric acid secretion and inflammation in the periphery, histamine serves an important function as a neurotransmitter in the central nervous system (CNS) (THURMOND, 2010).The histaminergic neurons originate from the tuberomammillary nucleus (TMN) of the posterior hypothalamus and send projections to most parts of the brain (Figure 2) The number of histamine-containing neurons is about 4000 in the rats whereas in human brain histaminergic neurons are more numerous (64,000) (HAAS; PANULA, 2003; THURMOND, 2010). The central histamine system is involved in many brain functions such as arousal, control of pituitary hormone secretion, suppression of eating and cognitive functions. The effects of histamine in the brain are mediated via four

histamine receptors (H1-H4), of which H1-H3 are highly expressed (THURMOND, 2010; CHANG et al, 2012; FLIK et al 2015).

Figure 2 - Histaminergic neurons and main projections in the human
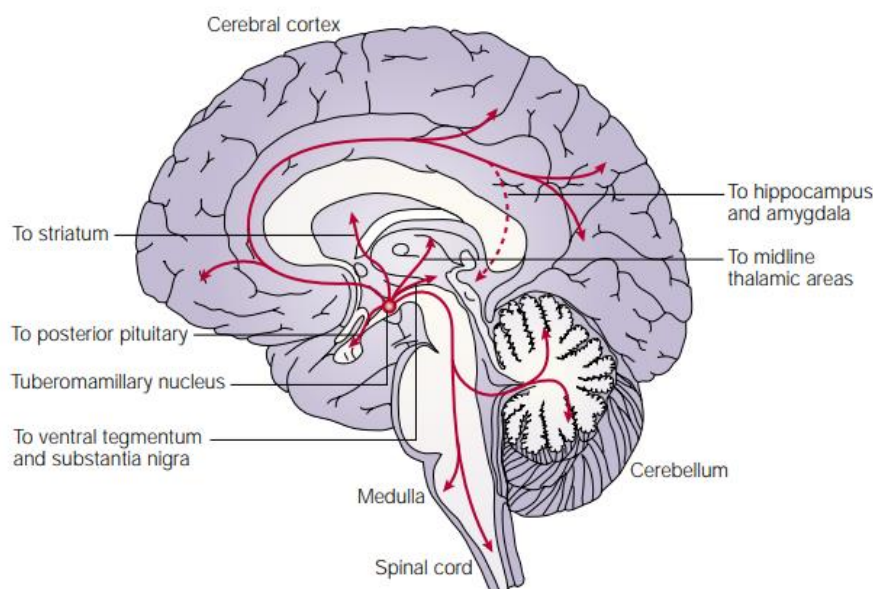
Source: HAAS; PANULA, 2003.

Three (H1, H2, and H3) of the four histamine receptors characterized by their molecular and pharmacological properties are widely expressed in the nervous system (HAAS; PANULA, 2003; HAAS et al. 2008; LEURS et al. 2009). The neuronal expression of H4 receptors has also been reported and their specific functions have begun to be studied (CONNELLY et al. 2009; FERREIRA et al. 2012). All four histamine receptors belong to the rhodopsin-like family of G protein-coupled receptors (CHAZOT et al. 2019). However, H3 are mainly expressed in the CNS and H4 are expressed in hematopoietic cells, indicating their function in neurotransmission and immunomodulation, respectively (CACABELOS et al 2016). The H3 is the high constitutive activity, which means spontaneous activity in the absence of histamine, and it is a recognized drug target for neuronal diseases, such as cognitive impairment, schizophrenia, sleep/wake disorders, epilepsy, and neuropathic pain (TILIGADA, 2016).

Not surprisingly, given its wide-ranging projections, histamine has been shown to be important in numerous brain functions. Histamine is also associated with a wide range of disorders, including cluster headache, disorders of consciousness, epilepsy,

addiction, essential tremor, and Parkinson's disease (PASSANI, PANULA; LIN, 2014). Despite its role in multiple processes and disorders, histamine has been less frequently studied compared to other biogenic amines, perhaps because it has traditionally been more difficult to measure (HAAS et al 2008). The ability to measure histamine has important clinical implications for the treatment of histamine-related disorders.

No disease entity has so far been linked specifically or selectively to brain histamine dysfunction. Additional factors must come into play to disclose the role of histaminergic dysfunction in disease. However, important changes in the peripheral and central levels of histamine occur in patients with different CNS disorders. These changes are particularly important in Alzheimer's disease, where histamine levels are significantly increased in most CNS regions. All these data together illustrate the potential role of histamine as a fundamental player in Alzheimer's disease-related neuroinflammation and other neuropsychiatric disorders (CACABELOS et al 2016).

Neurochemical monitoring has been generally obtained by one of two dominant techniques, microdialysis and electrochemical recording. Unlike microdialysis, electrochemical methods provide sub-second temporal and sub-millimeter spatial resolutions and can support direct measurement of analytic substrates at an implanted probe by detecting the oxidation and reduction currents of molecules (MICHAEL; BORLAND, 2007; CHANG et al 2012).

Thus, enzyme-modified biosensors have gained huge attention in the electroanalysis of histamine and other biogenic amines during recent years. Different types of electrochemical sensors with chemical modifications or with immobilized histamine oxidase and dehydrogenases have been described in several reports of histamine determination as we can see on the table 1 but they a focused in analysis of fish samples (HENAO-ESCOBAR et al, 2016; VERMA et al 2020). The development of stable histamine receptor with a capacity to detect low histamine concentrations (nM range) is an urgent need in the biomedical and diagnostics research.

Electrochemical biosensors have been described as more simple devices in the determination of histamine. The main problem of the described biosensors comes from the low enzyme selectivity and the high working potentials needed for operation, leading to an increase in the effect caused by the presence of different interfering species. Nowadays, the main efforts in the development of biosensors for histamine are focused on the improvement of their sensitivity, but also of their selectivity, based upon the specificity of the enzyme used (HENAO-ESCOBAR et al, 2016).

Therefore, in this work, a highly selective and specific enzyme is being used for the analysis of Histamine, namely histamine dehydrogenase from *Rhizobium* sp 4-9. This selected enzyme is pure active enzyme much more specific than the commonly used amino oxidases in the construction of biosensors for the determination of histamine and is not subject to substrate inhibition as its similar histamine dehydrogenase from *Nocordiodes simplex*.

Table 1 - Various electrochemical biosensors for biogenic amines determination (adapted from Verma *et a*l 2020)

ENZYME	ELECTRODE	MEDIATOR	IMMOBILIZATION	POTENTIAL	PH	LINEAR RANGE	DETECTION LIMIT
DAO: Diamine Oxidase	SPCE	-	Crosslinking with GA and BSA	-0.3V	7.2	1–75 mg/L	0.94 mg/L
DAO	LSG-nCu-CNC/DAO LSG-Cu-MFC/DAO	-	Crosslinking	+500mV	7.0	50–1.6mM	7.7 ± 2.8 µM 11.6 ± 2.6 µM
-	Cu-Pt electrode	-	-	200mV	10.0	1 to 750 mM15	0.33 mM
DAO	nPt/GPH/chitosan/SPCE –	-	Surface adsorption	+0.4 V	7.4	0.1–300 µM	2.54×10^{-8} M
Histamine dehydrogenase	HMD/TTF/SPCE	Tetrathiafulvalene-TTF	Crosslinking with GA and BSA	+130	6.8	8–60 µM	8.1 ± 0.7 µM
DAO-HRP	PS/MWCNTs/Fc-SPE	Ferrocene- Fc	Phase inversion technique	-50mV	7.5	3×10^{-7}– 2×10^{-5} M	1.7×10^{-7}M
DAO	Graphite electrode	Os (osmium) redox polymer	Crosslinking	-50mV	7.0	0.01– 0.5mM	5 µM

MAO: Monoamine Oxidase	MAO/HRP/SPCE	Hydroxymethyl ferrocene	Covalent binding	250 mV	9.3	0.4–2.4 µM	0.40 ± 0.04 µM
DAO	Pt/CSPE	-	Physical entrapment	0.35 V	7.4	0–60 ppm	0.65 ppm
DAO	platinum electrode	-	Covalent immobilization	600 mV	7.0	0–60 µM	0.5 µM
DAO DAO-HRP	platinum electrode	ferrocene monocarboxylic acid	Crosslinking with GA	+700mV	7.4	1 ± 100 µM 1 ± 100 µM	0.6 µM 0.1 µM
MAO	Screen printed - Pt	-	Crosslinking with GA and BSA	+ 600mV	8.5	0.17–20 µM	-
MADH	MADH-TCNQ carbon electrode	TCNQ	Adsorption	+200mV	7.5	0–200 µM	4.8 µM

PUO: Putrescine oxide, HRP: Horseradish Peroxide, GA: Glutaraldehyde, BSA: Bovine serum albumin, DAO: Diamine Oxidase, GPH: Graphene, nPt: Platinum nanoparticles, SPCE: Screen printed Carbon electrode, MAO: Monoamine Oxidase, HMD: Histamine dehydrogenase, PAO: Polyamine oxidase, CF: coconut fiber, CS: Chitosan, nZnO: zinc oxide nanoparticles, TCNQ: tetracyanoquinodimethane, MADH: Methylamine dehydrogenase, BSAO: bovine serum Amine Oxidase, SAMN@CrVI: stable core–shell nanostructures, GC:Glassy Carbon, MWCNTs: Multiwalled Carbon Nanotubes, PS: polysulfone, AuNP-PANSA AuE: gold nanoparticle-poly-(8-anilino-1-napthalene sulfonic acid modified gold electrode, LSG: laser scribed graphene, MFC: microfibrilated cellulose, CNC: nanocrystalline cellulose hydrogel, nano-Fe3O4: ironoxide nanoparticles, BAT: 2-[4,6-bis (aminoethylamine)-1,3,5-triazine].

1.2 Histamine dehydrogenase from *Rhizobium sp. 4-9*

The Histamine dehydrogenase from Rhizobium sp. 4-9 (HDR) was identified and partially characterized for Bakker and coworkers (2005) and showed remarkable substrate specificity and no activity toward putrescine and other biogenic amines, so it is useful for an enzymatic assay of histamine and does not use molecular oxygen as an electron acceptor.

The crystal structure was solved and released for Goyal and coworkers (2019 – to be published) but available PDB database. The HDR is an iron-sulfur-containing flavoprotein. HDR catalyzes the oxidative deamination of histamine to ammonia and imidazole acetaldehyde as we can see in the scheme 1. The enzyme is a homodimeric protein composed of subunits with a molecular mass of 76 kDa. Each subunit contains a covalently linked 6-S-cysteinyl flavin mononucleotide cofactor (FMN) and a [4Fe-4S] iron-sulfur cluster. Each subunit also possesses one adenosine diphosphate of unknown function (Figure 3). A homology analysis of amino acid sequences showed that HDR shared 54.5% identity with *rs*HDR (FUJIEDA et al., 2004), 39.3% identity with trimethylamine dehydrogenase from *Methylophilus methylotrophus* (TMDH, BOYD et al., 1992) and 38.1% identity with dimethylamine dehydrogenase from *Hyphomicrobium X* (DMDH, YANG et al., 1995).

Figure 3 - Crystal structure of the Histamine dehydrogenase from Rhizobium sp. 4-9 at 2.1 Å resolution*.*
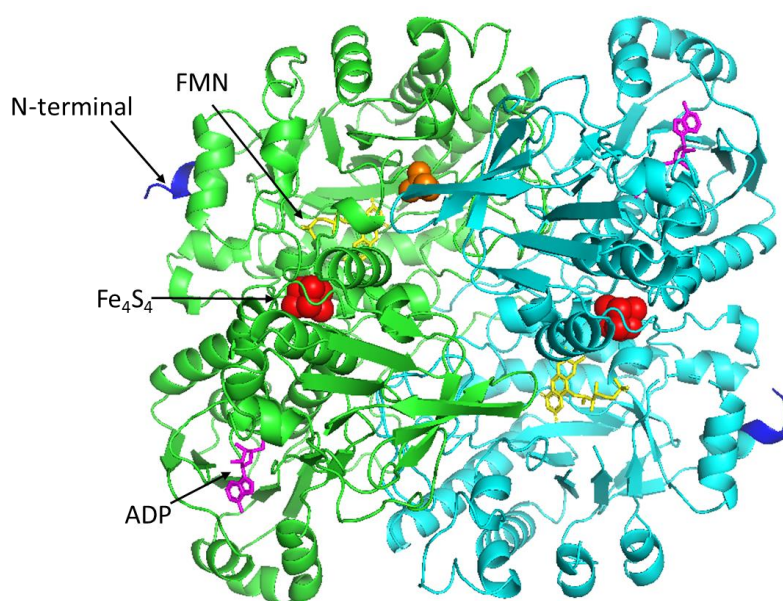
Source: GOYAL; LOVELL; RICHTER, 2019

Scheme 1 - Oxidative deamination of histamine to give imidazole acetaldehyde

$$\text{histamine} + H_2O \longrightarrow \text{imidazole acetaldehyde} + 2e^- + NH_4^+ + 2H^+$$
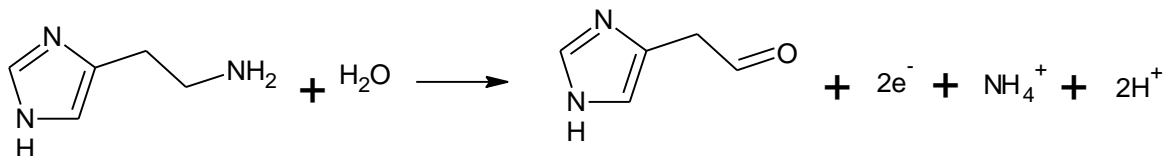
All these iron-sulfur-containing flavoproteins require three electrons per subunit for full reduction; two for reduction of FMN and one for the reduction of the [4Fe-4S] cluster. It has been considered that in these enzymes two electrons in the substrate are passed to the oxidized FMN (FMN$_O$) and two sequential single electron transfers occur from the fully reduced FMN (FMN$_R$) to the oxidized [4Fe-4S] cluster (FeS$_O$), and finally another two sequential single electron transfers are followed from the reduced [4Fe-4S] cluster (FeS$_R$) to electron acceptor. The physiological electron acceptor for *ns*HDR and HDR not identified. Several artificial electron acceptors such may be utilized in place of the physiological one, such as oxidized ferrocene derivatives (Fc$^+$). Therefore, the enzyme reduced with one equivalent amount of histamine per subunit corresponds to the enzyme composed of the two-electron reduced subunits. The two-electron-reduced form of *ns*HDR subunit is in equilibrium between two ultimate states: one involves the semiquinone form of FMN (FMNsq) and FeS$_R$ and the other involves FMN$_R$ and FeS$_O$. Thus, under steady-state conditions, for *ns*HDR and TMDH, at high substrate concentrations, the FMNsq is stabilized by the binding of a substrate cation and can no longer be oxidized by [4Fe-4S], leading to substrate inhibition (TSUTSUMI et al, 2009a; REED et al, 2010).

Scheme 2 - Electron transfer pathway

$$RCH_2NH_3^+ + FMN_O \longrightarrow FMN_R + RCHO$$

$$FMN_R + FeS_O \longrightarrow FMN_{SQ} + FeS_R$$

$$FeS_R + Fc^+ \longrightarrow FeS_O + Fc$$

*ns*HDR is much higher in the catalytic activity than HDR, but is strongly susceptible to substrate inhibition from histamine at high concentrations. Similar substrate inhibition is also observed for TMADH, which is inhibited by its natural substrate trimethylamine. In contrast, HDR does not suffer from such substrate inhibition (BAKKE et al, 2005). Therefore, HDR is a promising candidate as a catalyst in histamine sensors.

1.3 Electrochemical biosensor

According to an IUPAC recommendation in 2001, an electrochemical biosensor is a self-contained integrated device, which can provide specific quantitative or semi-quantitative analytical information using a biological recognition element (biochemical receptor) which is kept in direct spatial contact with an electrochemical transduction element. A biosensor can be used to monitor either biological or non-biological matrixes. Chemical sensors, which incorporate a non-biological specificity-conferring part or receptor, although used for monitoring biological processes, as the in vivo pH or oxygen sensors, are not biosensors. (THEVENOT et al., 2001). Electrochemical biosensors measure the current produced from oxidation and reduction reactions. The current produced can be correlated to either the concentration of the electroactive species present or its rate of production/consumption. The resulting electrical signal is related to the recognition process by target and analyte and is proportional to the analyte concentration (PERUMAL; HASHIM, 2013).

A typical biosensor usually contains: a bioreceptors that specifically bind to the analyte; an interface architecture where a specific biological event takes place and gives rise to a signal picked up by; the transducer element; the transducer signal is converted to an electronic signal and amplified by a detector circuit using the appropriate reference and sent for processing by, e.g., computer software to be converted to a meaningful physical parameter describing the process being investigated; finally, the resulting quantity has to be presented through an interface to the human operator. Biosensors can be applied to a large variety of samples including body fluids, food samples, cell cultures and be used to analyze environmental samples (GRIESHABER et al, 2008)

Amperometric devices are a type of electrochemical sensor, since they continuously measure current resulting from the oxidation or reduction of an

electroactive species in a biochemical reaction (LUPPA; SOKOLL; CHAN, 2001). Typically, the current is measured at a constant potential, and this is referred as amperometry. If a current is measured during controlled variations of the potential, this is referred as voltammetry. Furthermore, the peak value of the current measured over a linear potential range is directly proportional to the bulk concentration of the analyte, i.e. the electroactive species (LUPPA; SOKOLL; CHAN, 2001; THEVENOT et al., 2001). Since not all protein analytes are intrinsically capable to serve as redox partners in electrochemical reactions, these devices use mostly mediated electrochemistry for the electrochemical reaction of the analyte at the working electrode (GRIESHABER et al, 2008; PERUMAL; HASHIM, 2013).

Much interest is still focused on glucose biosensors both due to financial and scientific reasons, many improvements (generations) have been added since the 1960's. (BOLLELLA, GORTON, 2018). Nevertheless, nowadays, several kinds of commercial enzyme-based amperometric biosensors are accessible for measuring glucose, lactate, alcohol, etc., by using oxidases (i.e., glucose oxidase, lactate oxidase, alcohol oxidase, etc.) that oxidize their substrates producing hydrogen peroxide (H_2O_2) which is detected by the electrode. However, several aspects could be considered to have held back the emergence of additional breakthrough applications built on electrochemical biosensing (NGUYEN et al 2019).

Communication between a redox enzyme and an electrode has been a central theme and continues along the traditional three major electron transfer (ET) routes outlined in Figure 4, that is 1st, 2nd and 3rd generation biosensors. The electronic coupling between redox enzymes and electrodes for the development of analytical devices such as biosensors can be realized according to three mechanisms: (i) electroactivity of the substrate or product of the enzymatic reaction, i.e., H_2O_2, NADH, etc. (1st generation); (ii) mediated electron transfer (MET) with the use of redox mediators, small electroactive molecules (i.e., ferrocene derivatives, ferrocyanide, conducting organic salts, and quinones), which are able to shuttle the electrons between the enzyme active site and the electrode (2nd generation); (iii) DET between the redox center of the enzyme and the electrode surface (3rd generation), without mediators or co-substrates during the catalytic transformation of the substrate to the product. Commercial biosensors are mostly based on either 1st or 2nd generation biosensors, however, recent progress in bioelectrochemistry in combination with bioengineering of enzymes have shown that 3rd generation biosensors have now

reached the market to measure glucose (Figure 5) (BOLLELLA, GORTON; ANTIOCHIA, 2018; NGUYEN et al 2019).

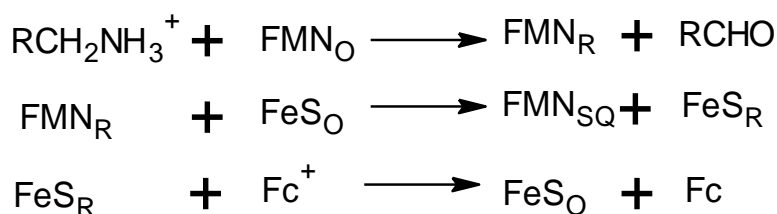**Figure 4** - Crystal structure of the Histamine dehydrogenase from *Rhizobium* sp. 4-9 at 2.1 Å resolution.

Source: BOLLELA; GORTON; ANTIOCHIA, 2018.

Figure 5: A commercial glucose biosensor based on DET

Source: http://www.directsens.com/
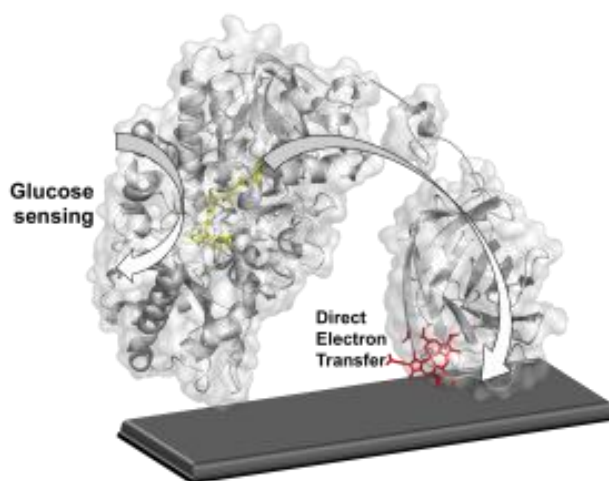
Adsorbed/immobilized mediators allow the making of reagent less biosensors possible (no freely diffusing mediator in solution), which is an obvious advantage compared to other 2nd generation biosensors that rely on the addition of a mediator to the sensing solution. Finally, 3rd generation biosensors based on DET offer a wide range of possibility to modulate the desired properties of the analytical device using protein modification either through gene or protein engineering techniques or new interfacial technologies making use of nanomaterials.

Although DET presents favorable characteristics for biosensors, only a few groups of enzymes are found to be capable of interacting directly with an electrode via a DET mechanism. This is because the redox centers of the enzymes are often buried within the protein structure in combination with a lack of an electron transfer pathway connecting the active site with the protein surface. An efficient DET mechanism has been demonstrated for a restricted number of enzymes. As for the dehydrogenases, DET communication has been reported also for a limited number of heme-containing enzymes, similar in their multicofactor composition (FAD, FMN, PQQ, or Moco in combination with heme) to dehydrogenase enzymes. However, these enzymes exhibit a medium-high reactions rate with molecular oxygen and are therefore denoted oxidases rather than dehydrogenases. Some even containing Fe-S clusters such as membrane bound succinate dehydrogenase (complex II in the respiratory chain), which shows DET properties both in its isolated "native" state as well as in its truncated form for which the heme containing part was removed. Among them, cellobiose dehydrogenase and fructose dehydrogenase are the most widely investigated for biosensing.

Recent advances in genetic engineering and molecular biology has allowed for the production of high-efficient and high specific recombinant enzymes, which are applied for the improvement of biosensor performance. The key technique is to increase the affinity of enzyme–substrate by facilitating substrate accessibility to the enzyme active site. In enzyme engineering, this purpose can be obtained using techniques such as site-directed mutagenesis or protein fusion.

Third generation sensors for histamine are not available yet but the DET of histamine dehydrogenase was already examined. Tsutsumi and Coworkers (2009) investigated the DET of histamine dehydrogenase from *Nocardioides simplex* (*ns*HDH) and that was achieved using a glass carbon electrode (GCE) modified with Ketjen Black (KB) with an average particle diameter of 39.5 nm, pH 9.0, although redox signal of the cofactors itself was not clearly for the enzyme itself, they observed a broad redox peak around 0.1 V *vs* SHE (standard hydrogen electrode). The pH dependence observed was similar to that of the redox potentials of the iron–sulfur cluster. Furthermore, since the flavin seems to be buried deeply in the cavity of the enzyme, it was difficult to directly communicate with electrodes. Therefore, they concluded that the [4Fe–4S] cluster site is the electron-donating site from *ns*HDH to electrodes and suggested that the side of [4Fe–4S] cluster in *ns*HDH faces the KB surface and the

flavin moiety as the catalytic center for the histamine oxidation would be toward the solution side for DET-active *ns*HDH on the electrode surface.

1.4 Current Approaches to Enzyme Immobilization

Currently, approaches to enzyme immobilization do not sufficiently address the need for highly bioactive and stable molecules with strong association to specific surfaces. Covalent modification utilizes harsh chemicals to form covalent bonds between the biomolecule and a surface. This provides a strong anchor for immobilization but has the potential to destroy the structure of the biomolecule; thus, limiting the bioactivity of immobilized molecules (BINAY et al, 2016; GREWAL; AHMAD; KHARE, 2017). For these reasons it is imperative that a biofriendly approach to the specific adsorption of biomolecules to inorganic surfaces is utilized. metallic surfaces for attaching any type of biomolecules.

Physical adsorption is one of the simplest ways to immobilize enzyme molecules onto support surfaces. However, controlling the interactions between the adsorbed molecule and the surface is difficult due to the weak and the nonspecific nature of the attachment process (GAUVREAU et al, 2004). Chemical coupling providing a more stable interfacial interaction is a widely used immobilization strategy (SHAO et al, 2010). Self-assembled monolayers (SAMs) have been the indispensable approach to functionalize the metallic surfaces for attaching any type of biomolecules. The covalent linkage between a surface and molecule is formed by monolayers of alkane chains containing different functional groups, dependent upon the surface chemistry of the support material and the biomolecule Specifically, utilization of the monolayers of alkane-thiolates, containing carboxylic acid or amine terminal groups, is well documented for gold surfaces (SARIKAYA et al, 2003; KRAULAND et al, 2007). Despite the enhanced stability of the coupling interaction, a major drawback of this approach is the low retention of enzyme activity due to the randomly introduced covalent linkages during the coupling reaction. Once formed, those covalent linkers establish very rigid attachments and prevent the immobilized biomolecules from positioning themselves toward their substrates and/or cofactors (TAMERLER; KHATAYEVICH; GUNGORMUS, 2010).

Due to the structurally anisotropic nature of the enzyme molecules, lack of orientation control prevents the utilization of the enzyme's full potential, especially for

bioelectric and biofuel cell devices (NAIKI et a, 2002) The realization of next generation hybrid devices integrated with biomolecules requires to develop more efficient immobilization methods. These techniques should provide better communication between the biological molecules and their solid surfaces built upon controllable interactions starting at the interfaces.

Over the last decade, combinatorial biology-based selection methods for solid binding peptides have gained attention as a novel alternative to the conventional surface functionalization and deposition techniques, owing to their ability to bring specific biomolecular recognition and binding properties onto inorganic surfaces (SASSOLAS; BLUM; LECA-BOUVIER, 2012). Moreover, the ease of genetic incorporation of these short sequences into any permissive site or the C- or N-terminus of an enzyme makes them an attractive option to the design of novel biomolecular systems featuring desired multifunctional properties (YANG et 2011; CENTINEL et al, 2013; YUCESOY et al, 2014; LEE et al, 2018; LEE et al, 2019). This opportunity presents many novel aspects to alter while designing next generation molecular systems through biological self-assembly. The biological nature of these short peptide sequences and their vast ability to create self-organized assemblies on a surface under physiological conditions make them highly desirable, when compared to their counterparts that may require higher temperatures and pH values, or other harsh reaction conditions.

Other peptides have potential binding properties for different types of surfaces. These peptides are expected to bind to surfaces by noncovalent interaction and can exhibit high affinity and selectivity. Some peptides are already used to anchor enzymes on different types of surfaces such as alkaline phosphatase on a gold surface (KACAR et al, 2009). Currently, these peptides are not well exploit to immobilize and orient redox enzymes on electrode surfaces, but they could provide a robust method to bind the enzyme at a different part of the protein. However, this binding method could also suffer from inhibition of the ET because of the length of the linker (HITAISHI et al, 2018).

One of the first reports associating gold-binding peptides (GBP) to proteins to bioelectrochemical applications was performed by Centinel and coworkers (2013) where they demonstrate an enhanced enzymatic activity and stability on a variety of gold surfaces ranging from nanoparticles to electrodes, by incorporating a GBP tag as the fusion partner into the N-terminus for *Bacillus stearothermophilus* L-lactate

dehydrogenase (*bs*LDH). The redox catalysis efficiency of the immobilized enzyme was detected using cyclic voltammetry analysis in enzyme-based biosensors for lactate detection as well as in biofuel cell energy systems as the anodic counterpart. Before that, it was demonstrated an immobilization method for biosensor applications through site-specific interactions between GBP-fused organophosphorus hydrolase (GBP-OPH) and gold nanoparticle-coated chemically modified graphene (Au-CMG) (YANG et al 2011).

More recently, Lee and coworkers (2018) describe a design and construction of a synthetic glucose dehydrogenase (GDH; α and γ subunits) combined with a gold-binding peptide at its amino or carboxy terminus for direct contact between enzyme and electrode. In this case, the fusion of site-specific binding peptide to the catalytic subunit (α subunit, carboxy terminus) of the enzyme complex enabled apparent direct electron transfer (DET) across the enzyme−electrode interface even in the absence of the electron-transfer subunit. The catalytic glucose oxidation current at an onset potential of ca. (−) 0.46 V vs Ag/AgCl was associated with the appearance of an flavin adenine dinucleotide (FAD)/FADH$_2$ redox wave. Lee and coworkers (2019) in a further report showed a significant enhancement of direct electric communication across enzyme-electrode when using gold nanoparticle (AuNP)-modified electrode.

In this study, we genetically engineered histamine dehydrogenase from *Rhizobium sp.* 4-9 to couple with cyclic gold-binding peptide as fusion enzyme with chimeric properties. Herein we use this novel enzyme system to probe how immobilization with a solid binding peptide tag affects catalytic activity of the fusion enzyme for potential biosensing applications.

2 AIMS

2.1 General Aims

Use recombinant DNA techniques to incorporate affinity peptides into histamine dehydrogenase, evaluate the affinities of peptide-protein constructs on gold surfaces as well as their orientation with respect to the surface and verify the efficiency of direct or mediated electron transfer between the enzyme constructs.

2.2 Specific Aims:

o	Incorporate affinity peptides into histamine dehydrogenase protein. Design gene blocks encoding peptide-protein conjugates, obtain commercially, and incorporated into plasmid vectors.

o	Over-express the protein in *E.coli.* C and N-terminally labeled HDH expressed in soluble form.

o	Perform TEV cleavage of the solubility tags and purify using standard lab protocols.

o	Determine the catalytic activities of constructs using established enzyme assays to assess any effect of peptide incorporation on enzyme

o	Identify an electron acceptor and evaluate its performance as mediator to the system with a higher turnover.

o	Analyze the purified peptide-protein constructs for their binding affinity to gold surfaces through SPR, SPR and AFM experiments.

o	Analysis of the immobilized enzyme on gold electrodes as a sensor using voltammetric and amperometric techniques.

3 MATERIALS AND METHODS

3.1 Materials

The pMCSG7 vector was prepared previously in the lab and used as a cloning and expression vector, *Escherichia coli* strain XL10 gold cells and BL21 (DE3) pRARE were selected as the host organism for both studies, respectively. Ampicillin and bacterial media supplements were obtained from Sigma– Aldrich. Chemicals used in buffer preparations, Histamine dihydrochloride, bovine heart cytochrome C were purchased from Sigma–Aldrich. 1,1- Ferrocenedimethanol was purchased from Santa Cruz Biotechnology, Inc. Binding studies were performed using gold-coated SPR chips (GE Healthcare, USA).

The Phosphate buffer (10 mM, pH 7.4), used in most of the assays, was prepared by dissolving 0.72g (Na_2HPO_4) and 0.18g (KH_2PO_4) in 500 mL of deionized water and the pH was corrected by adding NaOH or HCl solutions.

3.2 Cloning of CT-cAuBP-HDH and NT-cAuBP-HDH fusion enzymes

The cyclic gold binding peptide (cAuBP, CPGWALRSSIRRQSYGPC) + (SSGSSG) linker was inserted into either of the N-terminus or C-terminus of the Histamine Dehydrogenase from *Rhizobium sp* gene by performing inverse PCR on the ligation independent vector pMCSG7 (Figure 6). An additional GB1 solubility-tag was added to the construct to enhance the obtained protein. The CT-cAuBP+linker and NT-cAuBP+linker gene blocks were obtained commercially from the company Integrated DNA Technologies IDT and used for cloning with HDH using ligation independent cloning method. The CT-cAuBP-HDH and NT-cAuBP-HDH encoding DNA sequences were constructed using Polymerase Chain Reaction (PCR) by primers specifically designed to add the cyclic gold binding peptide and the linker to the N-terminus and C-terminus of the protein coding region, respectively. PCR was conducted using gBlocks® Gene Fragments Protocol: Megaprimer RF Cloning (Table 2) in the T100 Thermal Cycler PCR machine.

Figure 6 - Schematic diagram of vector construction of the (A) GB1-CT-cAuBP-HDH and (B) GB1-NT-cAuBP-HDH fusion proteins

A
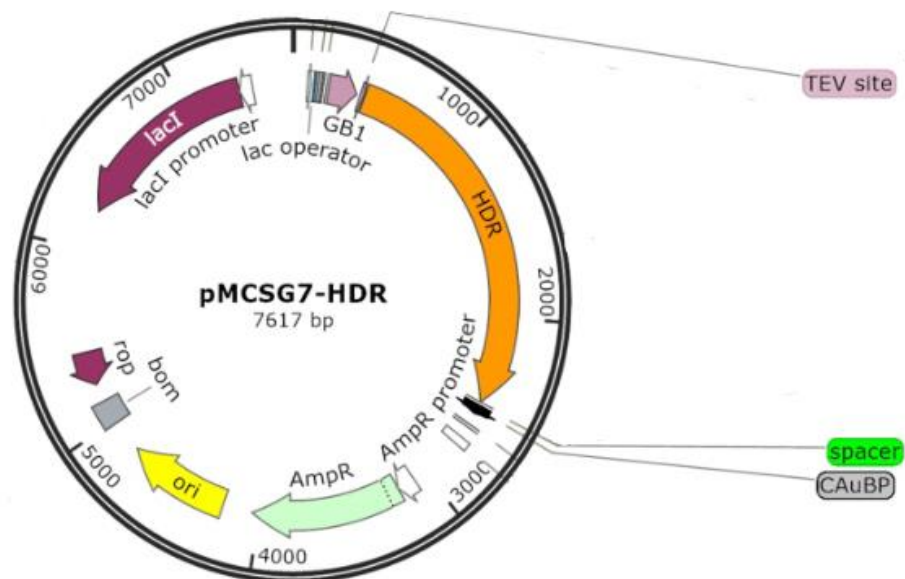
B
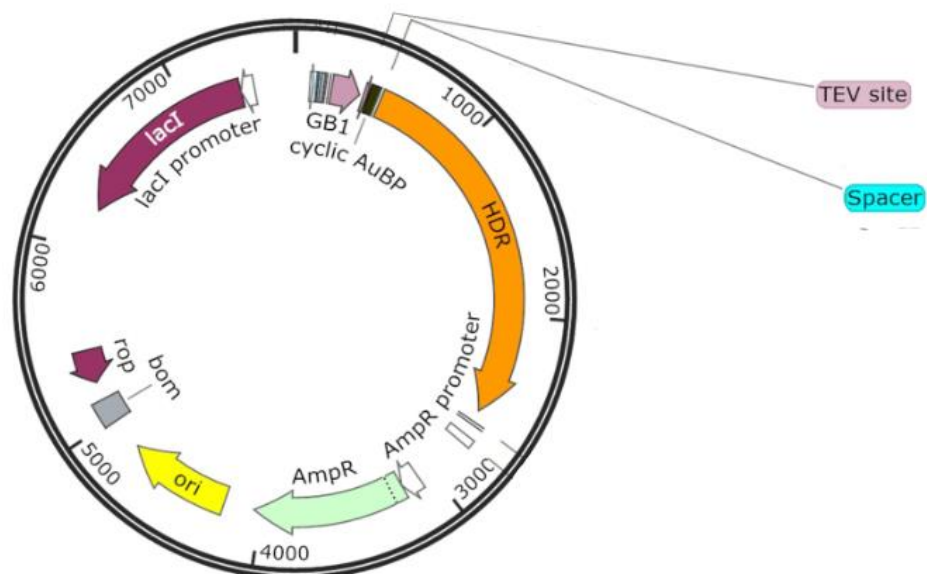
Table 2 - PCR protocol using gBlocks® Gene Fragments Protocol: Megaprimer RF Cloning protocol

Component	25 µl REACTION	Final concentration
5X Q5 Reaction Buffer	5 µl	1x
10 mM dNTPs	0.5 µl	200 µM
Wt-HDH Template DNA	0.5 µl	<50ng
gblock gene fragment	10 µL	
Q5 High-Fidelity DNA Polymerase	0.5 µl	0.02 U/µl
Nuclease-Free Water	To 25 µl	

The resulting PCR amplified protein coding sequences were transformed using XL10 gold cells and incubated overnight at 37°C. A few of the resulting colonies were inoculated to overgrow at 37°C shaker incubator for further DNA extraction, following the QIAprep® Spin Miniprep Kit protocol. The DNA concentration was measure using NanoDrop 200c spectrophotometer (Thermo Scientific) and the samples were sent to have the sequence checked and confirmed by ACGT, Inc.

After DNA confirmation, the resulting constructs were transformed into the expression host *E. coli* BL21 (DE3) pRARE cells via chemical transformation.

3.3 Over - Expression of CT-cAuBP-HDH and NT-cAuBP-HDH fusion enzymes

Cells were first grown overnight at 37°C in 10 ml of Luria Bertani (LB) media, containing carbenicillin and Chloramphenicol. Next, the overnight culture was inoculated into fresh 1L LB media with glycerol and $MgCl_2$ and incubated at 37°C until it reached an optical density (OD600) 0.6-0.8. The culture was induced with isopropyl β-D-1-thiogalactopyranoside (IPTG) addition to a final concentration of 0.1 mM and glycerol and the culture was incubated overnight at 15°C with constant agitation (250 rpm). Cells were then harvested by centrifuge for 10 min, 5000 rpm and 4°C and re-suspended in potassium phosphate buffer (50 mM KH_2PO_4, 150 mM NaCl, 5 mM imidazole, pH 7.4) and then kept in the -80°C overnight. After that the cells were

thawed the next day, 5uL DNAse treatment for 10 minutes on ice and sonicated at 30% amplitude, for 2 mins. With 2sec on and 10 sec off cycle. Finally, resulting cell lysate was centrifuged for 1h at 4°C at 20000 rpm and the supernatant solution was reserved for further purification.

3.4 Purification of CT-cAuBP-HDH and NT-cAuBP-HDH fusion enzymes

The similar affinity purification method, i.e. nitrilotriacetic acid (Ni-NTA) metal-affinity chromatography, was used to purify the CT-cAuBP-HDH and NT-cAuBP-HDH. Pre-packed NiNTA column was first equilibrated with potassium phosphate buffer (50 mM KH2PO4, 150 mM NaCl, TCEP 250µM and 5 mM imidazole at pH 7.4) and then the total protein containing supernatant solution was loaded into the column and mixed under rotation for 1h in the fridge. After that, non-specifically bound proteins were removed by potassium phosphate buffer (50 mM KH_2PO_4, 150 mM NaCl, TCEP 250µM, 20 mM imidazole at pH 7.4). Proteins of interest were eluted by increasing the imidazole concentration in the potassium phosphate buffer up to 250 mM. Finally, the purification process was confirmed by the sodium dodecyl sulfate polyacrylamide gel electrophoresis (SDS-PAGE) analysis. The GB1-tag was cleaved using a 1:10 w/w of TEV protease.

3.5 Sodium Dodecyl Sulfate Polyacrylamide Gel Electrophoresis (SDS PAGE)

The polyacrylamide gel electrophoresis in the presence of sodium dodecylsulfate (SDS-PAGE) was performed using 12% polyacrylamide gels (NuPAGE™ Bis-Tris Mini Gels 12 %) and MES Buffer 2x. Aliquots of purified enzymes were applied to the gel and electrophoresed in a XCell SureLock™ Mini-Cell gel apparatus. The molecular weights of proteins were determined by comparing the migration of the protein with those of molecular weight markers (Sigma Chemical, USA). Proteins were stained using Coomassie blue dye (InstantBlue ™).

3.6 Affinity tag (GB1-tag) removal from enzymes

After purifying the enzymes, Bradford readings at 595 nm were measured in order to calculate the total enzyme present. Then TEV enzyme in mL was added based on the total amount of enzyme present in the collected volume in a 1:10 ration of TEV enzyme: protein. Along with this DTT (to 5 mM) and EDTA (to 1 mM) were added, and

the mixture kept overnight at 4°C for the TEV cleavage reaction to take place. After this, the protein was desalted using a Sephadex G-50 spin column in order to remove DTT and EDTA. The desalted protein was applied to a reverse Ni-NTA column to remove the GB1 and the His tag that gets attached to the Ni-NTA while the protein devoid of the His tag elutes from the column. The yield was calculated using Bradford assay. The protein was then stored in 20%(V/V) glycerol in -80°C for future use.

3.7 Enzyme activity measurements

Purified enzymes were desalted on a Sephadex G-50 spin column equilibrated with 10 mM potassium phosphate, pH 7.4 and the protein concentration determined by Bradford assay.

The steady-state enzyme activity measurements were carried out at 25°C and/or 37°C in a reaction mixture containing 10 mM Phosphate buffer at pH 7.4 containing-, 2.5 mM ferricineumdimethanol (FcDM$^+$), 10 μM to 2 mM histamine, and 0.1 μM enzyme in a total reaction volume of 1 mL. The initial (first 20 sec) rate of FcDM$^+$ reduction was measured as the change in absorbance at 640 nm in a Cary 50 spectrophotometer. Kinetic parameters were obtained from a non-linear regression analysis using the *Graphpad Prism* software and fit to a Michaelis-Menten kinetic model. Reaction rates were converted into apparent unimolecular turnover rates using the calculated extinction coefficient of FcDM$^+$ (ε_{640}= 247.73 cm-1 * M-1) and the enzyme molecular weight (76 kDa). Measurements were reproduced three times and all assays were performed in triplicates.

The kinect assay was also performed with bovine heart cytochrome C cytochrome C and histamine (2-10 μM), by following changes in absorbance at 550 nm extinction coefficient of (ε_{550}= 29500 cm-1 * M-1) under the same conditions used for the FcDM$^+$ assay.

3.8 Localized Surface Plasmon Resonance Assays

Citrate-capped AuNPs (Ted Pella, INC) were incubated with serial dilutions of HDH and CT-cAuBP-HDH proteins. Citrate-capped 15-nm AuNPs, which exhibit a characteristic LSPR maxima at 519 nm wavelength, demonstrated a red shift upon replacement of citrate by protein molecules. Binding and interaction properties of the fusion proteins to AuNP surfaces were compared with respect to their measured LSPR

band shift. The measurements were performed using a TECAN Safire UV–Vis spectrometer microplate reader.

3.9 Atomic Force Microscopy studies of surface bound HDR

To prepare enzyme electrodes, gold templates were used. 100 µL (0.001, 0.05 and 0.1 µM) of synthetic (CT-cAuBP-HDH) or native HDH were pipetted onto the gold substrate surfaces and incubated for 60 min. The gold plates with immobilized enzyme were rinsed several times with buffer and pH adjusted water. After that, the surfaces were, thoroughly blow-dried with argon. All surface topography images were taken with a multimode scanning probe microscope (Nanoscope IIIA, Digital Instruments CA) using tapping mode. For tapping mode images, diamond like carbon coated (DLC) Tap 300 probes (spring constant of 40 N/m) from Budget sensors were used. All AFM images were analyzed using NanoScope Analysis 1.5 software by Bruker Corporation. For high-resolution imaging, cantilevers with a nominal radius of 5 nm were used to assess the topography of enzyme immobilized on the Au surface.

3.10 Surface binding kinetics measurements

Binding kinetics of CT-cAuBP-HDH and wt-HDH enzymes were performed using a four channel BiaCore T200 SPR instrument (GE Healthcare). After establishing a stable baseline signal by flowing 10 mM TRIS-Cl (pH 7.5) or 20 mM sodium phosphate buffer (pH 7.4) over the surface, enzyme solution at given concentrations were flowed across the surface, and their adsorption was monitored. BiaCore gold chips were utilized. The temperature within the flow cell of the SPR was kept at a constant 25°C by a temperature sensor. All the solutions used were introduced to the flow cell at a rate of 10 µl/min with 1800s of association and dissociation time. Regeneration solutions such as 6M Guanidine pH 7.4 or pH 10.0, with a flow rate of 30µL/min were utilized in SPR studies. In our data analysis, the Langmuir isotherm model will be used to calculate the association (k_a), dissociation (K_d), and equilibrium (K_{eq}) constants of the adsorption/desorption process. All the proteins were sized in SEC (size exclusion chromatography) before using for SPR.

3.11 Oxidation of 1,1- ferrocenedimethanol (FcDM) by soluble bilirubin oxidase

The oxidation of the ferrocene derivative (1,1- ferrocenedimethanol; Fw = 246.09 g/mol) was adapted from a method described by Luong et al, 1995 (patent 5,432,274). The bilirubin oxidase (9.1 units/mg) was added to a dissolved solution of 1,1- ferrocenedimethanol (5 mM) and the solution turned from yellow to green and finally blue, an indication of its oxidized form (scheme 3 and Figure 7). The development of the blue color was monitored at the absorption maximum for $FcDM^+$ at 640 nm.

Scheme 3 - Enzymatic oxidation of 1,1- ferrocenedimethanol by bilirubin oxidase.
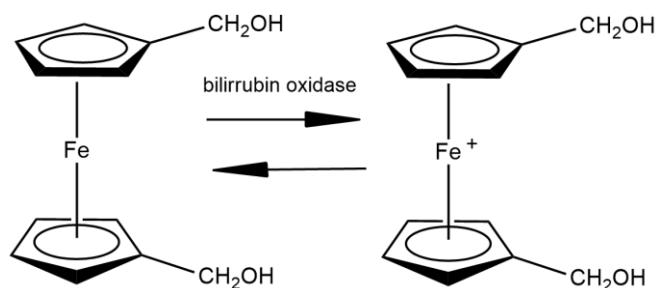
Figure 7 - Oxidation of 1,1- ferrocenedimethanol (yellow) to its oxidized form (blue)

Source: Author, 2019

The reaction was performed in 40 mL of Phosphate buffer 200 mM pH 5.8. The oxidation of FcDM (5 mM, 40 ml) to $FcDM^+$ using ~1 unit of bilirubin oxidase (100 µL of 1mg/mL solution) with constant air bubbling, the reaction proceeded to completion in about 30 min. After complete reaction, the enzyme was destroyed by lowering the pH to 2.5 (with HCl) and after 2 min incubation, the pH was readjusted 7.4 (with NaOH). The product was stored at room temperature.

3.12 Electrochemical measurements

Cyclic voltammetry (CV) experiments were performed using a CHI model 410 potentiostat (CH Instruments, Austin, TX) and a conventional three-electrode cell (Figure 8). Ag/AgCl (KCl) was used as the reference electrode, Pt as the auxiliary electrode and gold (diameter = 2 mm), as the working electrode. The CV for enzyme−electrode characterization was performed in 10mM Phosphate buffer pH 7.4 with different amounts of histamine at scan rates of 20 mV s^{-1}.

Initially, the possibility of direct electron transfer between the redox site of the enzyme and the electrode was tested-, without any external acceptor, so after enzyme immobilization through the parameters on table 3, the histamine was added at different amounts (0.1 to 1.25 mM) and the voltammograms recorded. After that, the oxidized ferrocene derivative was tested as an electron acceptor to the system either with the enzyme in solution or on the electrode. The FcDM^{+} was added to the electrochemical cell and the changes caused when the biogenic amine was added were recorded.

Amperometry experiments were performed using a CHI model 7104 potentiostat (CH Instruments, Austin, TX) and rotating disc electrode apparatus, an Analytical Rotator and ASR speed control (Pine Instrument Company), 500 rpm. A conventional three-electrode cell. Ag/AgCl (KCl) was used as the reference electrode, Pt were used as the auxiliary electrode and gold rotating disc electrode (diameter = 7 mm, as working electrode. Measurements were conducted in Phosphate buffer pH 7.4.

The amperometry technique was used to obtain the current response after each histamine addition in a preliminary study, to find the parameters for the best response and viability of our sensor under development. Using the rotating disk electrode (RDE) system allows control of the mass transfer rate,-so that the electrode activity can be quantitatively analyzed in sufficient reproducibility (BARD; FAULKNER, 2001).

Figure 8 - Schematic representation of electrochemical celll
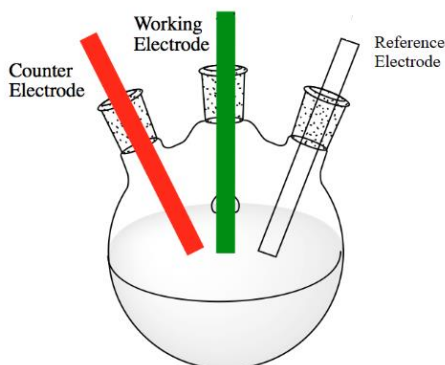
Source: Google images.

3.12.1 Immobilization of CT-cAuBP-HDH and WT-HDH on gold electrodes

Different approaches were performed to find the best immobilization method (Table 3), various amount of enzyme was tested on the electrode (0.5 to 10 µM). The immobilization of the fusion protein was carried out in phosphate buffer (pH 7.4) solution at room temperature. In brief, 100 µL of CT-cAuBP-HDH solution was added on top of the gold rotating disc electrode or 10 µL when the static gold electrode was tested and allowed to it for 1-2h to allow site-specific affinity of cAuBP with gold. In addition, the control WT-HDH was prepared by the same protocol as for the CT-cAuBP-HDH.

Table 3 - Parameters of different immobilization approaches for the fusion and wild-type enzymes on gold electrode.

| Technique	Volume dropped	[Enzyme]	Approach	Time
CV	10 µL	10 µM	Dry off with N_2 or at room temperature	~1h
Amperometric	100 µL	0.5 to 10 µM	Wash off after some time	1h; 2h

4 RESULTS AND DISCUSSION

4.1 Genetically engineered CT-cAuBP-HDH and NT-cAuBP-HDH fusion enzymes

A selected and characterized cyclic gold binding peptide (cAuBP) (HNILOVA et al 2008) was used as a fusion partner to HDH. The cAuBP peptide sequence was inserted between the GB1-tag and the C- or N-terminus of the wt-HDH coding region using a SSGSSG (Serine-Serine-Glycine–Serine-Serine-Glycine) spacer to allow for efficient peptide display. The resulting engineered protein thereby ensures that the gold binding peptide region is freely exposed to the environment without any restriction on its conformation as well as any potential interference with the enzyme. To purify the expressed recombinant protein with high yields, we also employed a GB1 solubility tag-based approach. The protein G B1 domain (GB1, 6.2 kDA, 56 residues) (HUTH et al. 1997; ZHOW; WAGNER, 2010) has been shown to increase the yield of soluble proteins. In previous protein expressions attempts, the cAuBP-enzymes was expressed in a non-solubilized form, into bacterial inclusion bodies. In this study, the GB1 tag was removed using the TEV protease after the protein was purified. The resulting protein remained soluble.

A schematic representation of cAuBP incorporated the HDR, showing the spatial organization of the GB1 tag, the TEV cleavage site and gold binding peptide regions is presented in Figure 9 (A). The plasmids encoding cAuBP-HDH were successfully expressed in E. coli XL10 gold cells, and the correct DNA sequence was confirmed by ACGT, Inc.

The resulting constructs were successfully transformed into the expression host *E. coli* BL21 (DE3) pRARE cells strains and purified using Ni-NTA matrices under native conditions. The purity and molecular weights of the expressed proteins were analyzed by SDS–PAGE (Figure 10). The protein bands indicating NT-cAuBP and CT cAuBP-HDH were observed approximately at approximately 77 kDa, which is the expected molecular weights for both enzymes following the inclusion of new sequences.

Figure 9 - (A) The final enzymes construct and (B) a schematic representation on the gold surface of the cAuBP fusion protein.
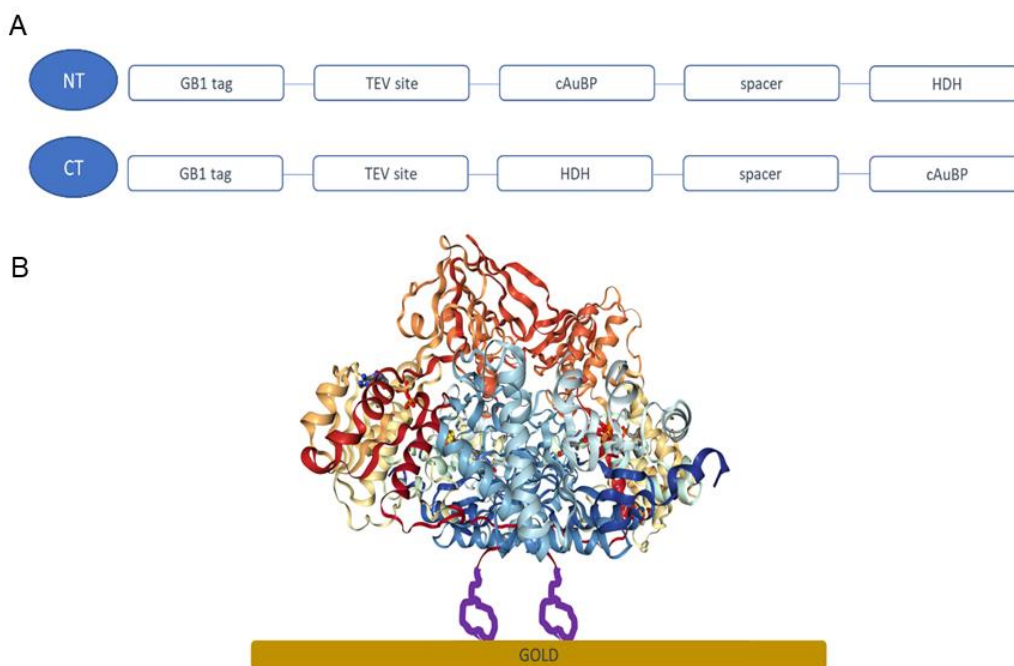
Source: Author, 2020.

Figure 10 - SDS-PAGE image of purified enzymes after removal of GB1 tag; CT and NT-cAuBP-HDR
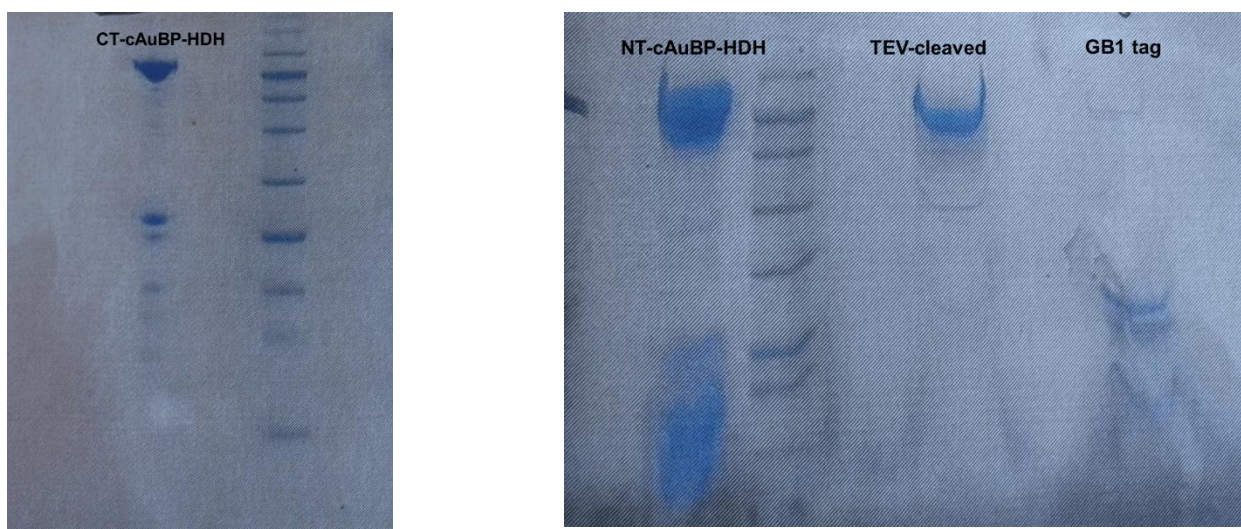
Source: Author, 2019.

4.2 Enzyme activity measurements

After the successful expression and purification processes, the catalytic activity of the wild-type and engineered enzymes were analyzed. The wild-type HDH shows

histamine concentration dependence of the steady-state enzyme kinetics in the presence of Fc$^+$ as an artificial electron acceptor at pH 7.4 (Figure 11). The enzyme exhibits high substrate selectivity and no substrate inhibition even at high turnover rates (k_{cat}>127s^{-1}) observed using soluble ferricenium (Fc$^+$) substrates, unlike the closely related Histamine Dehydrogenase from *Nocardioides simplex.* The calculated enzyme kinetic parameters k_{cat}, which indicates the turnover rate of substrate to product, and K_m or k_{50} (the Michaelis constant), which describes an enzyme's affinity for its substrate, are provided in Table 4.

Figure 11 - Steady-state kinetic analysis of the reaction of WT-HDH (0.1 µM) and histamine (10 µM to 2 mM). In phosphate buffer at pH 7.4 with, -2.5 mM FcDM$^+$ as acceptor, 25^{0}C
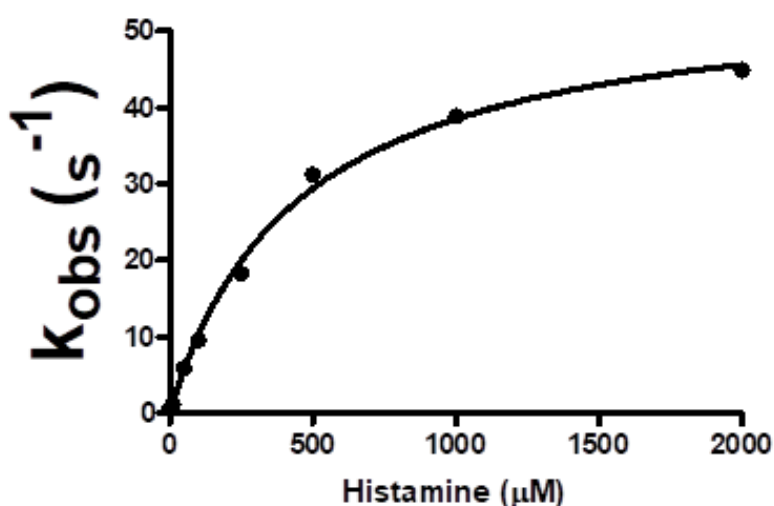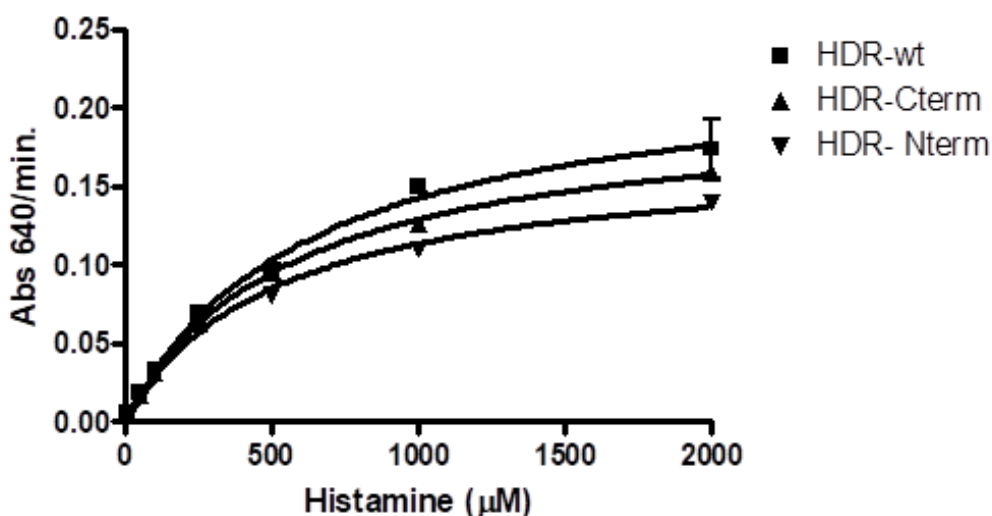

Source: Author, 2019

Table 4 - Kinetic parameter for the wild-type and fusion enzymes. The K_{50} value represents the concentration of histamine giving half maximum reaction velocity.

HDH enzyme	K_{50} (µM)	K_{cat} (s^{-1})	Temperature (°C)
Wildtype	1369	127.3	37
Wildtype	451.9	55.93	25

Source: Author, 2019

The most commonly used immobilization approaches explored so far and described in the literature result in a significant loss of catalytic enzymatic functionality, potentially due to the randomly introduced covalent attachment methods used random attachment approaches involving direct protein adsorption on the electrode surface. In our case, we have added a new functionality to the enzyme by way of introducing affinity peptide to attain surface functionalization in a manner that will potentially enable control over the orientation of the enzyme on the electrode surface. We first tested if the enzymes would retain its catalytic activity following the introduction of the new gold binding peptides into the enzyme structure. The k_{cat} value obtained for both the N-and C-terminally placed peptides showed small decreases relative to wild type enzyme without a tag (Figure 12 and table 3) indication that the tags do not greatly interfere with enzyme function.

Figure 12 - Comparison of affinity peptide and the wild type enzyme activity obtained by the (FcDM+) consumption at 640 nm. 0.1 µM enzyme, histamine (10 µM to 2 mM). Phosphate buffer at pH 7.4, 2.5 mM FcDM$^+$ as acceptor, at 25°C.

Source: Author, 2019

In contrast, Kacar and coworkers (2009) observed, when measured in solution, that the enzyme activity of the wild type Alkaline phosphatase (AP) was approximately fifteen times higher than the 5GBP1-AP fusion protein containing a gold binding peptide repeat on the N-terminus. Centinel and coworkers (2013) observed that the presence of the AuBP2 slightly decreased the enzyme activity of the L-lactate

dehydrogenase (LDH) both in terms of catalytic activity and enzyme efficiency (k_{cat}/K_m) and similar results were found for the formate dehydrogenase fusion enzyme from *Candida methylica* (cmFDH–AuBP2) where the k_{cat} obtained for the cmFDH–AuBP2 was very close to that of cmFDH wild-type. Furthermore no significant difference in the substrate affinities K_m/k_{cat} of cmFDH–AuBP2 and cmFDH were observed (YUCESOY et al 2014).

Interestingly, both AP and LDH, when immobilized on gold surfaces, showed higher enzymatic activity than the wild-type proteins (KACAR et al, 2009; CENTINEL et al, 2013). However, this may not necessarily be a general trend for all enzymes and the effect of tags introduced on either end of an enzyme mays is likely to differ on a case-by-case basis. Prediction of the optimum enzymatic performance based on tag placement may be aided through genetic search for a permissive placement site (MANOIL; TRAXLER, 2000),-which would provide the position for genetic fusion of the inorganic-binding peptide on to the molecule with the highest retained enzymatic activity while also allowing solid binding functionality of the fusion (KACAR et al, 2009).

The natural electron acceptor for this enzyme is unknown, so we have measured spectrophotometrically the activity with several small-molecule redox acceptors including possible natural acceptor including cytochrome C, azurin, ferrodoxim and cytochrome b from cellobiose dehydrogenase. Of these, only Cytochrome C acted as an acceptor bur with a very slow rate as indicated in Figure 13 and table 5. Of several small molecule mediators tested, ferriceniumdimethanol provided the most robust turnover (127.3 s^{-1}, 37°C). Since, ferriceniumdimethanol is not available commercially in its oxidized form, it has it was oxidized before the experiment, following an adapted method that promotes the 1,1-ferrocenedimethanol oxidation by bilirubin oxidase (LUONG et al, 1995). An advantage of using this ferrocene derivative is its solubility in aqueous media in both reduced and oxidized forms, in contrast to the commercially available ferrocenium hexafluorophosphate that was precipitated when reduced following the same kinetic analysis performed here.

Figure 13 - Steady-state kinetic analysis of the reaction of WT-HDH with Cytochrome C as acceptor. The reaction mixture contained 0.1 µM enzyme, 10 µM to 2 mM histamine. Phosphate buffer at pH 7.4.
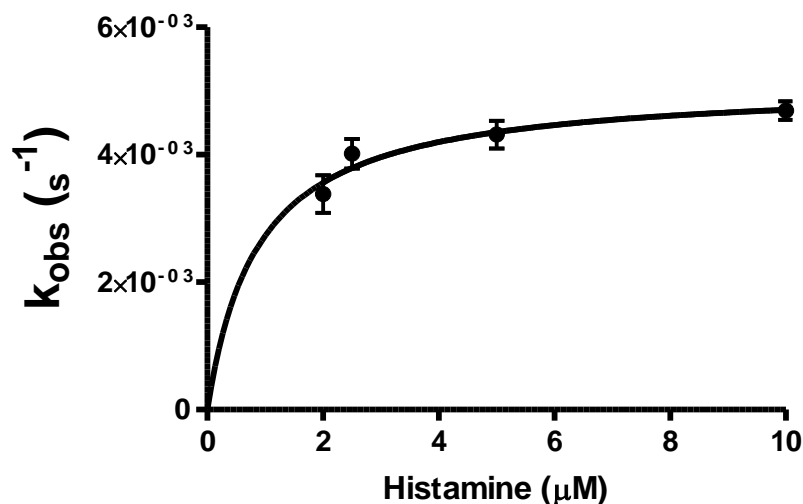
Source: Author, 2019

Table 5 - Kinetic parameter for the wild type using Cytochrome C as acceptor data at 37°C

CYTOCHROME C DATA AT 37 C	
ET	1 µM
K_{CAT}	5.18×10^{-3} s^{-1}
K_{50}	0.88 µM
V_{MAX}	1.2×10^{-2}

Source: Author, 2018

The calculated K_{50}, for histamine varied with the acceptor indicating that reoxidation of the flavin was rate-limiting. The micromolar K_{50} and the relative high turnover with FcDM$^+$ are well suited to measure the concentration of histamine that is found in tissue samples, thereby should work effectively on a biosensor for measuring biologically relevant histamine levels in the CNS. Studies performed elsewhere (BAKKER et al, 2005; SATO; HORIUCHI; NISHIMURA et al, 2005; HENAO-ESCOBAR et al, 2016) have shown that the enzyme is inactive toward a long list of biological amines. This group has also observed (data not published) that the enzyme

has zero measurable activity with serotonin as substrate, an important consideration when measuring histamine concentration in the brain.

4.3 Localized Surface Plasmon Resonance (LSPR)

Due to their localized surface plasmon resonance characteristics, gold and silver nanoparticles exhibit unique optoelectronic properties commonly used in biomedical sciences and engineering. Localized surface plasmon resonance has been recognized as a label-free bio-sensing method that is sensitive and robust. While these inherent properties make LSPR a platform technology to be utilized in a wide range of applications, controlling the interfacial biomolecular interactions remains a challenge. Local refractive index changes around the metallic nanoparticle can be measured by the sensitivity of the surface plasmon frequency. Then, we investigated the assembly and binding properties of CT-cAuBP-HDH onto gold, nanoparticles using the LSPR method.

AuNPs were prepared and incubated with the fusion proteins for 2 h. Next, the absorbance spectra were recorded to calculate spectral peak shifts for each sample. Spectral shifts indicate an altered surface structure and size when AuNPs are successfully functionalized because LSPR peak wavelength and bandwidth of AuNPs critically depend on size, shape, and the surrounding medium refractive index and temperature.

The optical absorption spectrum of AuNPs shows a LSPR peak at 318 nm (light blue line, Figure 14 (A-F) and the LSPR shifts were analyzed at twelve different protein concentrations. The Figures 14 (E and F) show that the absorption spectrum of hybrid protein shows 6-nm red shift in the LSPR peak of AuNPs from 518 to 524 nm at 0.05 µM and at that same concentration the wilt type protein's shift was from 518 to 521 nm what would suggest that the synthetic protein binds to AuNP with a higher affinity than the control, however the increase on molar concentrations resulted on higher shifts for the wild type protein as showed in the Figure 14-C, suggesting that the WT-HDH binds to AuNP with superior affinity than the CT-cAuBP-HDH in higher concentration.

Higher protein concentration adsorption resulted in a higher red shift, supporting the consistent mass increase. The result found here suggests that a stable protein layer was formed on the surface of the nanoparticle following the incubation with the increase in the nanoparticle size (Figure 14 A-F). Metal nanoparticles, when they are

functionalized with a biomolecule, have been observed to result in UV–Vis absorbance red shifts and are stimulated by the spacing and plasmonic coupling between nanoparticles.

The adsorption of the control protein was considerably high for the gold surface and similar to that genetically modified, which was not expected and that can be attributed to non-specific interactions that are possibly caused by the presence of surface exposed residues. As is well-known in the protein structure literature, it is not just the chemical but also the physical structure of the protein (i.e., its 3-dimensional conformation in space) that equally significantly affects its binding and molecular recognition characteristics (TAMELER, et al 2006).

Figure 14 - Localized surface plasmon resonance (LSPR) spectra of protein functionalized AuNPs. Spectral peaks collected after 2 h of incubation with CT-cAuBP-HDH and HDH protein (0.0001 to 4 µM).
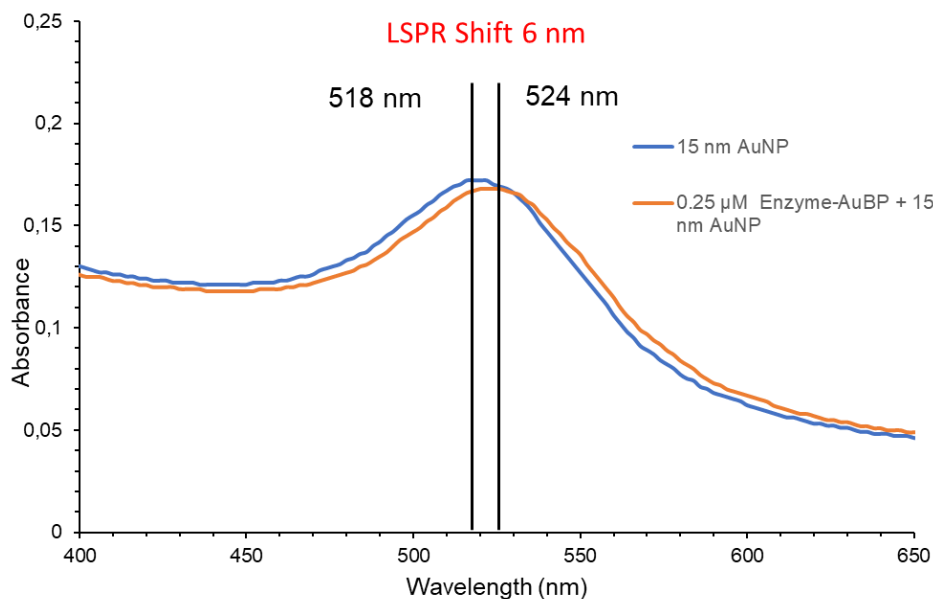
A
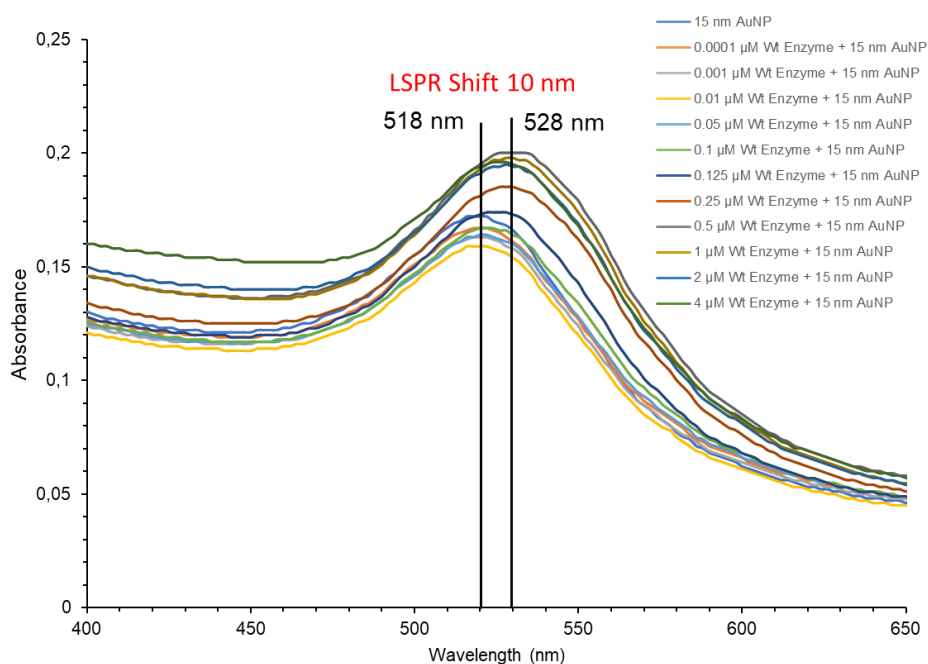
B
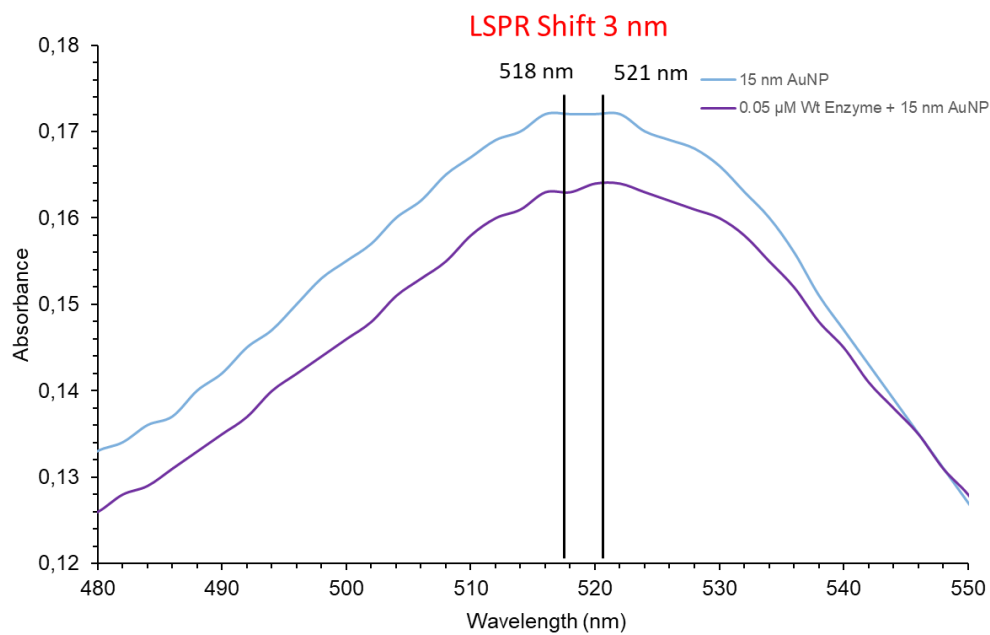
C
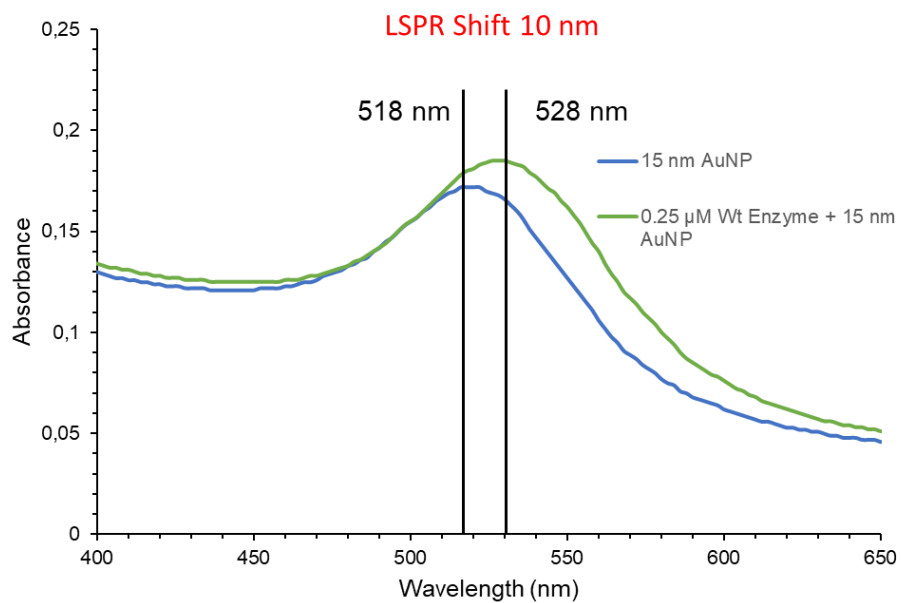
D
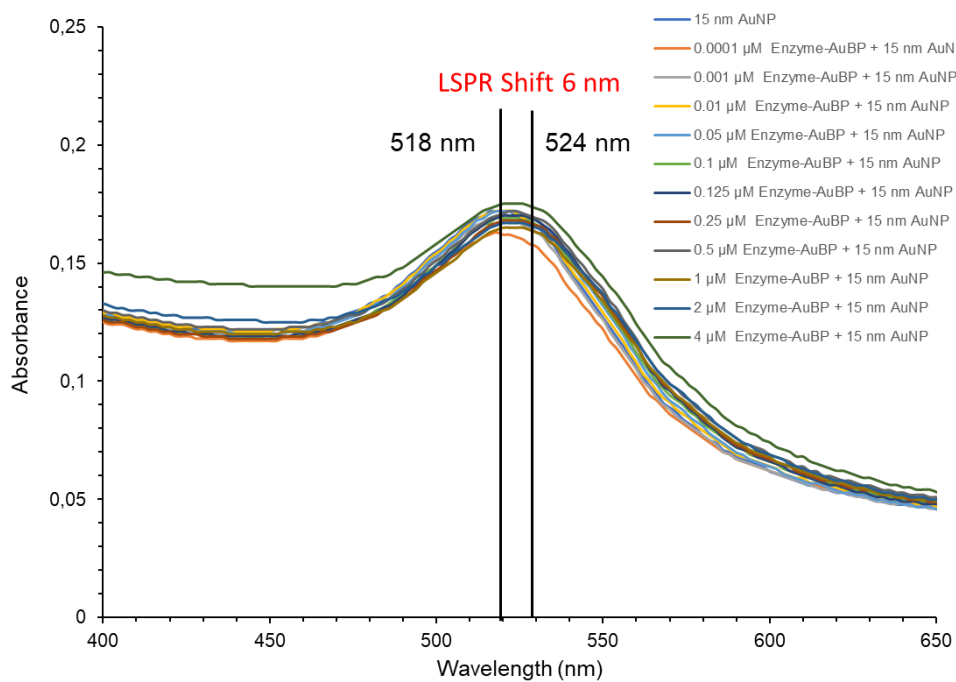


E
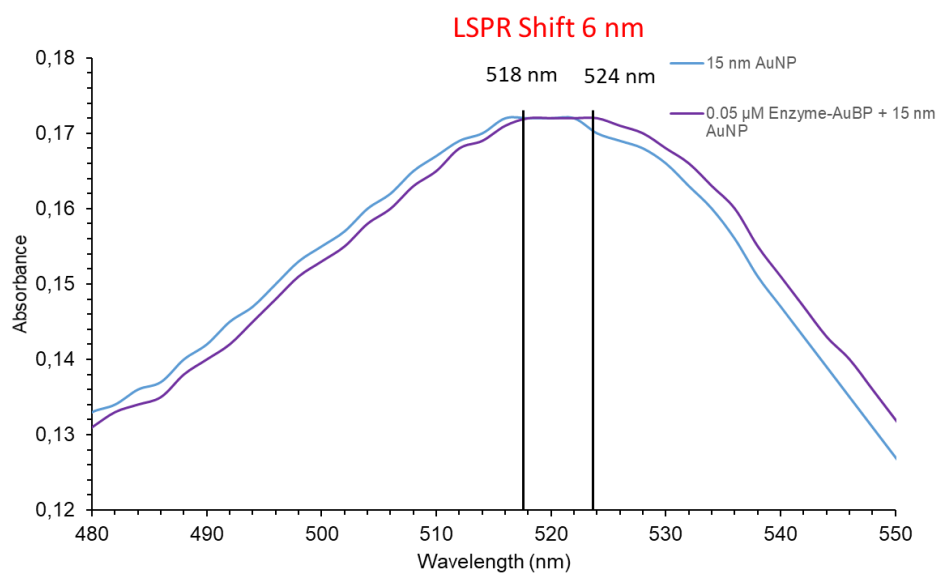
F

Source: Author, 2019

4.4 Atomic Force Microscopy studies of surface- bound HDH

The directed immobilization and the resulting morphology of the WT-HDH and the CT-cAuBP-HDH on gold substrate were examined using non-contact mode AFM. Consequently, the enzymes were introduced on template-stripped gold (TSG) surfaces, thus the following AFM images in Figure 15-17 represent coverage states of the wild type enzyme and the fusion enzyme at different concentrations ranging from 0.01 to 0.1 µM protein solution exposed over 1h incubation and after being washed several times to minimize non-specific bind. As a result, in the Figure 15 the gold substrate was exposed to 0.05 µM wild type enzyme and obtained surface coverage of the 744±190 (Molecules/µm^2). The enzyme is the little shine dots on the gold templates, the bigger dots are enzyme aggregates or impurities. When exposed to CT-cAuBP-HDH at the same concentration the surface coverage was slightly bigger, 755±182 (Molecules/µm^2). Upon closer inspection in Figure 15 and 16 A, it can be recognized that the CT-cAuBP-HDH units are slightly more spread on the surface than the wild-type.

As we can see in Figure 16 (A-C) and summarized on table 6, with the increase in the enzyme concentration higher was the bind of the fusion protein, as previously observed to the 3rGBP1 (triply repeated Gold Bind Peptide), where the AFM images

were produced at seven different concentrations ranging from 2–2320 nM exposed over this time period, as a result, the coverage data suggested that, under equilibrium conditions, that peptide appeared to obey simple Langmuir adsorption (SO; TAMELER; SARIKAYA, 2009). The Figure 17 shows isolated single molecules of the CT-cAuBP-HDH on gold template.
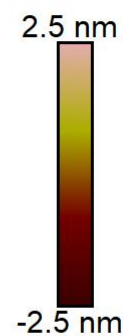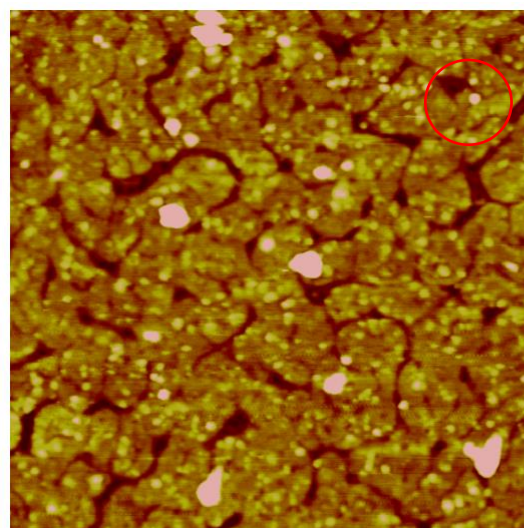
Figure 15 - Atomic force microscopy observation of the WT-HDH assembly on Template Stripped Gold, after 1h incubation with 0.05 µM enzyme.
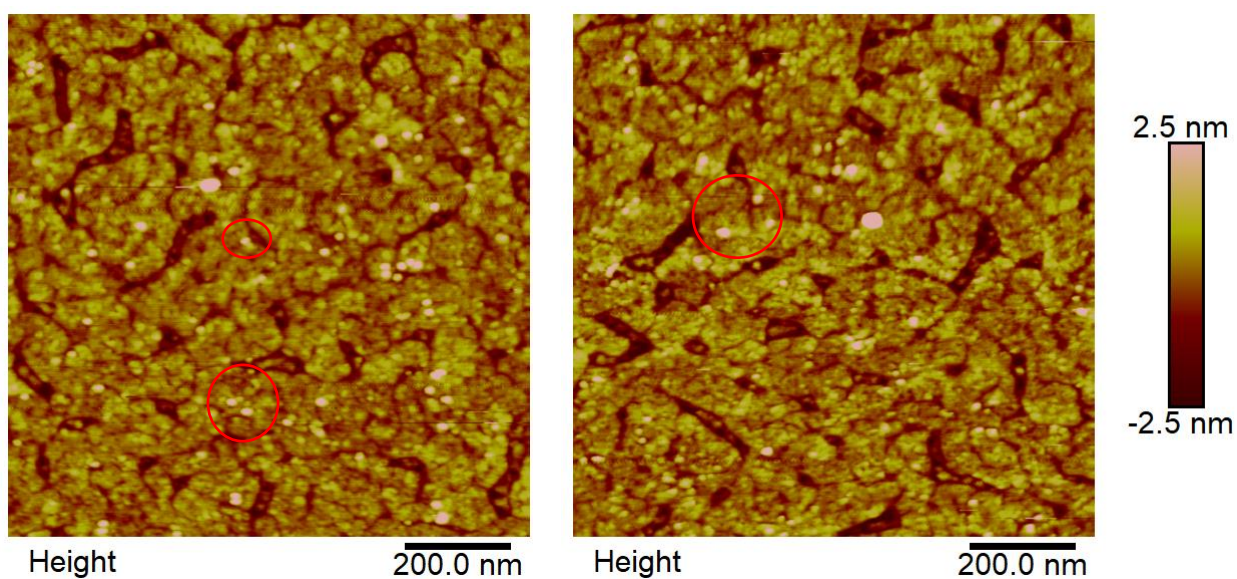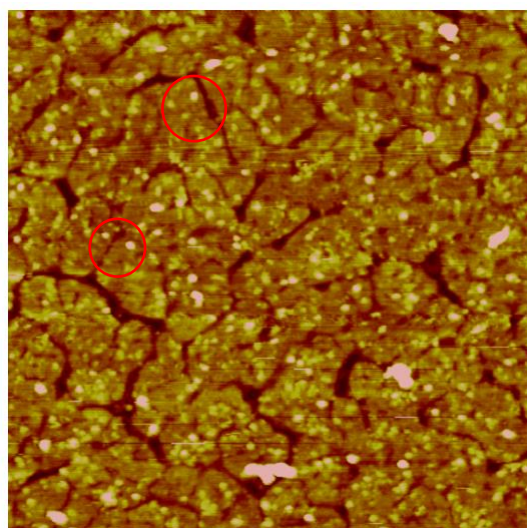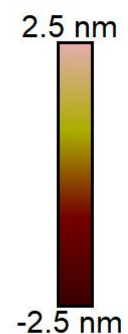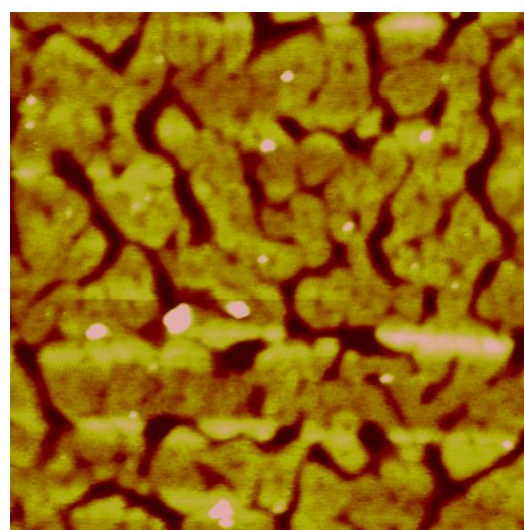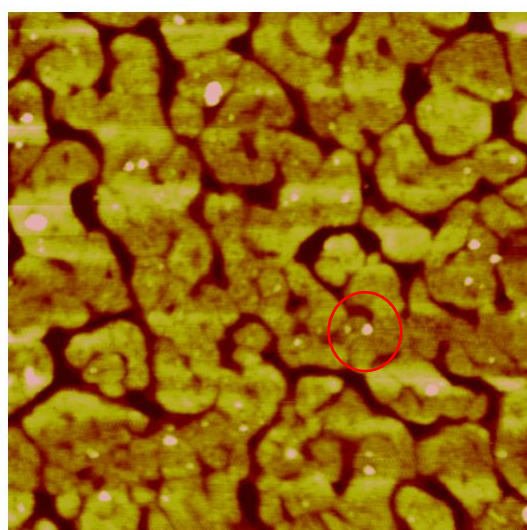

Source: Author, 2019

Figure 16 - Atomic force microscopy observation of the CT-cAuBP-HDH assembly on Template Stripped Gold, after 1h incubation with (A) 0.05 µM (B) 0.01 µM and (C) 0.1 µM.
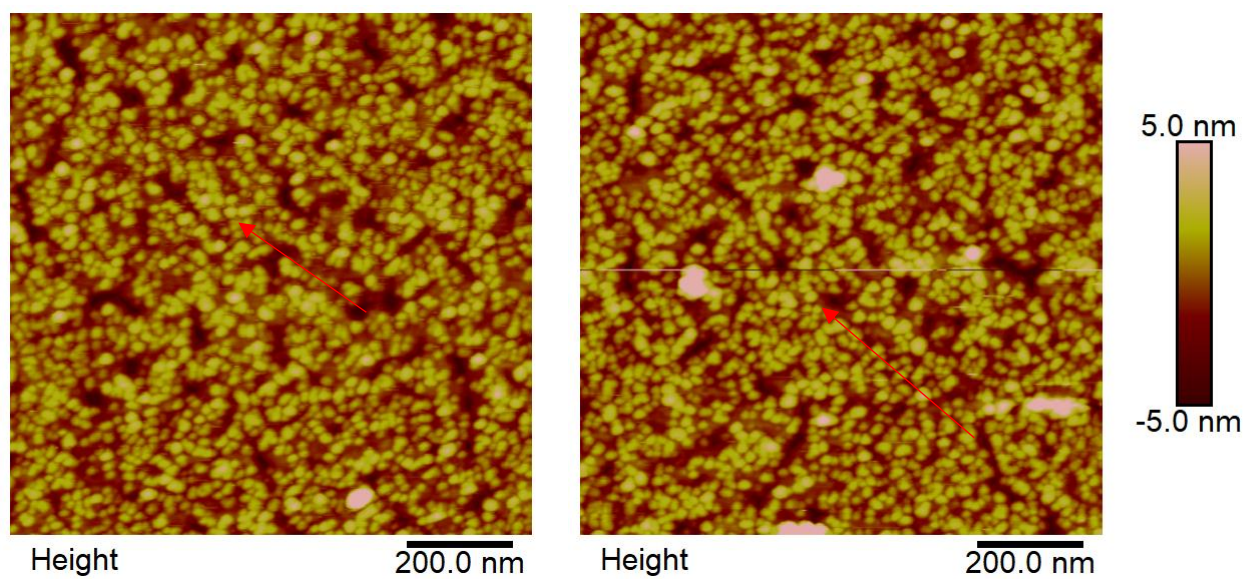
C
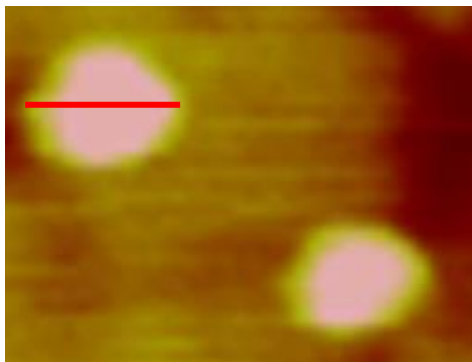
Table 6 - Surface coverage to the CT-cAuBP-HDH on TSG.

CT-cAuBP-HDH (μM)	Surface coverage (Molecules/μm^2)
0.01	33±5
0.05	744±190
0.1	2116±184

Figure 17 - Isolated single molecules of the CT-cAuBP-HDH on TSG, after 1h incubation and washed several times
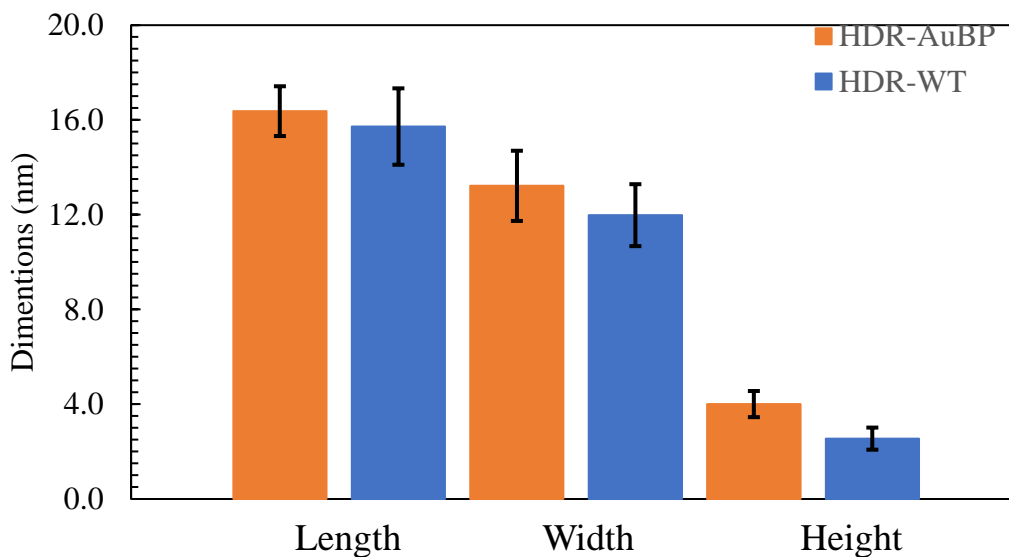

Source: Author, 2019

The dimensions of the immobilized enzymes obtained from AFM characterization are comparable with the molecular dimensions of the protein (Figure 18), length and width were done for 25 molecules while the height was calculated for 50 molecules and the error bars are standard deviations. Shown in Figure 19, it reveals step heights in the films which correspond to increments of 2.5 and 4.0 m from the gold surface after incubation with WT-HDH and CT-cAuBP-HDH, respectively which means that peptide-fusion protein is 1.5 nm higher than the wild type, similar to the previously observed values (SO et al, 2009), and recently by Kamathewatta and coworkers 2020, which has used the same gold-peptide tag sequence. The dimensions reported here were recorded with the same tip under similar imaging conditions to allow direct comparison to produce the AFM images from both samples, the discrepancy in feature sizes was not seen to arise from experimental artifacts, such as tip convolution. This dimension is indicative of fusion enzyme assembled to the surface due to gold-binding peptide, although the wild type also shows a strong non-specific bind. These findings suggests that both enzymes bind differently on gold surfaces, and that the presence of the cAuBP holds the protein away from the surface in a more vertical orientation even though the similar surface coverage.

The recognition mechanism underlying such affinity has not been studied in detail, and it is not clear how the wild-type and fusion protein direct the recognition and interaction processes on the Au surface or what molecular features would enable self-associative behavior. Various residues or domains of a given protein may interact with a given solid. These interactions are often non-specific and result in protein adsorption with loss of function as well as a loss of long-term stability (ZHANG; CASS, 2001). The AFM images to the AP and 5GBP1-AP (KACAR, 2009) showed that both the wild-type

and the hybrid construct bind to the gold regions of the patterned surface. However, they differ the molecular packing density (high number density of enzyme immobilized) and more homogenous in the case of 5GBP1-AP.

Figure 18 - Dimensions of WT and cAuBP tagged HDR on TSG Dimensions of WT and cAuBP tagged HDR on TSG

Source: Author, 2019

Figure 19 - Height of HDR wild type and fusion protein on TSG
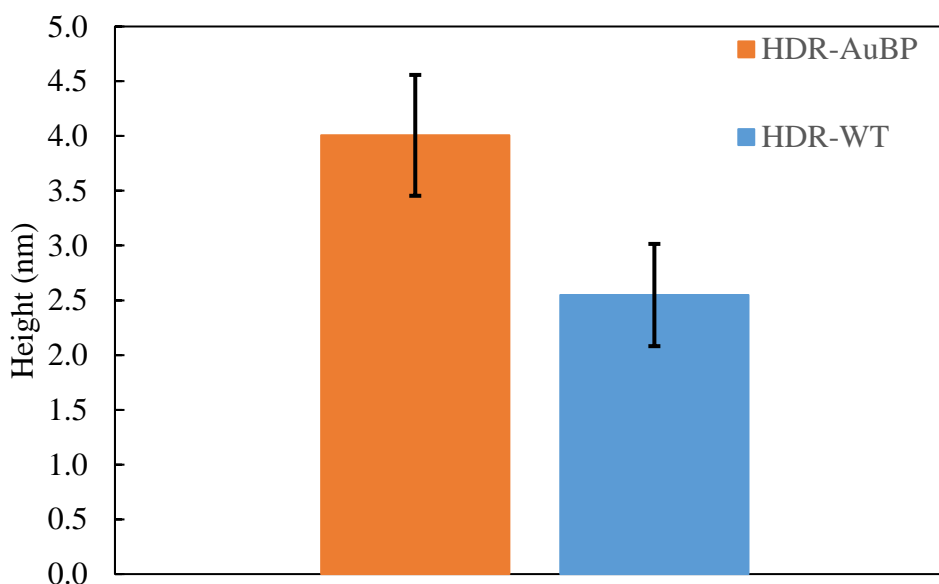
Source: Author, 2019

4.5 Electrochemical studies

The histamine dehydrogenase from the gram-negative bacterium *Rhizobium Sp.* 4-9 is comprised of a homodimer of 76 kDa monomers each containing one covalently attached flavin mononucleotide and one Fe_4S_4 iron sulfur center that shuttles electrons between the reduced Flavin and an external acceptor. Here, we are interested in developing a biosensor to measure histamine levels in tissues, especially the brain. The concept is to engineer a coupled enzyme system that contains the cAuBP-HDH with a covalently bound external acceptor that carries electrons from the flavin/FeS of HDH to an electrode surface.

### 4.5.1 Cyclic Voltammetry technique

Although direct electron transfer (DET) is observed for some enzymes (typically heme and blue copper proteins) on electrode surfaces, this is not the common trend because it is very hard to achieve electrochemical communication with electrodes. According to Marcus theory calculations, the maximum distance of electron tunneling between donor and acceptor was estimated to be 20 Å (HITAISHI et al 2018). Actually, this is the distance which is reached through complex formation between the active sites of two interacting proteins. Modification of electrode surfaces can facilitate interaction of proteins with transducers, thus facilitating DET and/or electrocatalysis. This modification of electrode interfaces usually consists in conferring a suitable overall charge or specific functional groups (SILVEIRA; ALMEIDA; 2013).

Peptide-based molecular linkers have been explored as a way to control the enzyme orientation on the surface via biomimetically designed biofunctional interfaces and inorganic surface-specific peptide tags are promising candidates to be an integral part of metal or semiconducting surfaces by bringing either recombinant redox enzymes or reconstituted apoenzymes into direct contact with the electrodes. (CENTINEL et al, 2013). Currently, these peptides are poorly used to immobilize and orient redox enzymes on electrode surfaces, but they could provide a robust method to bind the enzyme at a different part of the protein. However, this binding method could also suffer from inhibition of the ET because of the length of the linker (HITAISHI et al 2018).

Direct electron transfer of purified N-terminus, C- terminus cAuBP-HDH fusion protein and wild-type HDR was investigated after protein immobilization on the

electrode (Figure 20 and 21), although we could observe a wave stating at 0.15 V in the figure 20 that was not reproducible on other assays (Figure 21-A) or with the NT-cAuBP-HDR. Thus, the gold-binding peptide did not allow the proper orientation which would enable the contact between the redox center of the enzyme and the electrode. The expected electrochemical behavior is present in the Figure 20, observing an increase in the oxidation process of the redox center of the enzyme. The wave showed around -0.3 V is the oxygen dissolved in the solution once the system was not isolated.

Figure 20 - Direct electron transfer assay CT-cAuBP-HDH before (●) and after histamine addition 0.5 (●), 0.75 (●) and 1mM (●).
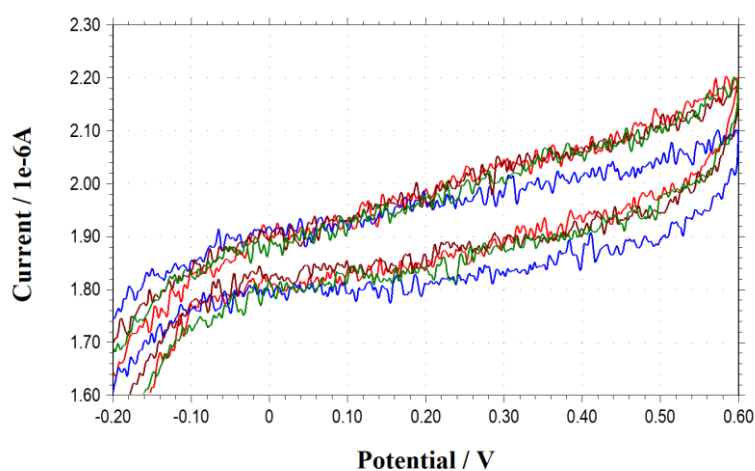
Source: Author, 2019.

Figure 21 - Direct electron transfer assay (A) CT-cAuBP-HDH, (B) NT-cAuBP-HDH.,
before (●) and after histamine addition (●) 0.5 mM

A

B
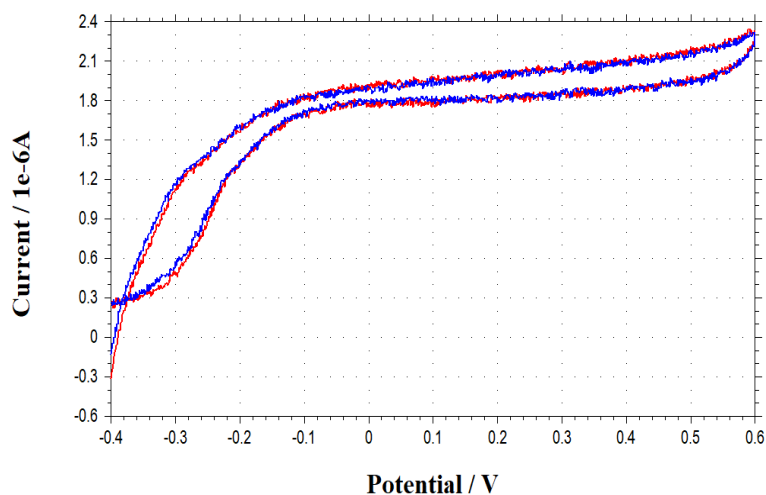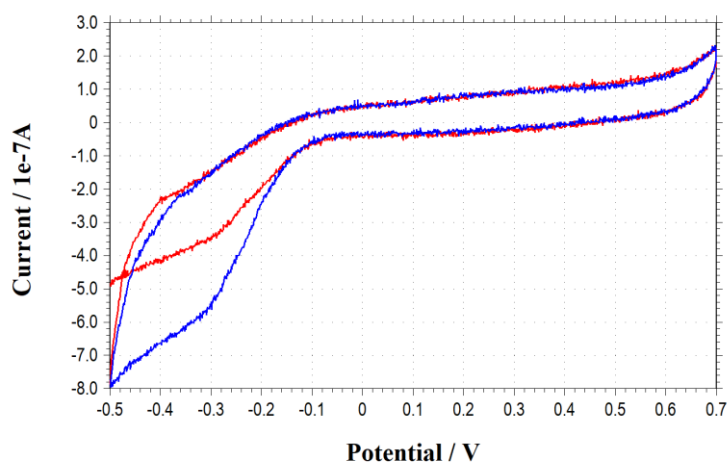
Source: Author, 2019

There is little work in the literature investigating the use of gold-binding peptides
(GBP) associated with proteins for biosensors applications. However, it is still not clear
how the association of the binding peptide could facilitate DET and the nature of the
binding with gold electrodes. All of the reports until the present day attached the GBP
into the N or C-terminus of the enzyme but as showed here this strategy cannot always
guarantee DET, It should be interesting to have possibilities of mutation at other

targeted parts of the enzyme, eventually closer to the active site, or at any locations on the enzyme surface in order to relate the position at which the enzyme is immobilized to the ET rate (HITAISHI et al 2018). Each protein has a unique structure and there is consequently no all-encompassing "one fits all" solution for orientation control. The quest for optimum performance using biofunctionalization methods needs to be expanded to fully utilize the wide functional repertoire of biological systems conducting diverse functions in living organisms (CENTINEL et al, 2013).

Nevertheless, when studying enzyme electrocatalysis a common approach is the use of redox mediators, i.e., small electroactive molecules that can easily interact with the protein's redox centers and consequently exchange electrons between electrodes and the biocatalyst. In this way, mediators can provide the means to follow and measure enzymatic reactions by electrochemical methods.

Electrical contact of oxidoreductases that lack DET with electrodes can be established by means of a reversible redox couple, one of the forms of which serves as a co-substrate of the enzyme. Over the years, much work has focused on identifying efficient mediators to ensure enzyme wiring to electrodes. These are generally organic compounds, for example viologens, phenazines, quinones, tetrathiafulvalene, and tetracyanoquinodimethane, or metal complexes, such as osmium, ruthenium, ferrocene, and derivatives (SILVEIRA; ALMEIDA, 2013).

The figure 22 shows the electrochemical behavior of ferriceniumdimethanol (FcDM$^+$) and HDR, in the presence and absence of histamine at gold bare electrode in Phosphate Buffer pH 7.4. In the absence of histamine, the reversible electrochemical behavior of FcDM$^+$ was observed on bare gold electrode (green line, Fig. 22). After histamine addition the anodic peak current increased dramatically and the cathodic peak current decreased, characteristic of catalytic process and reflecting the electron transfer from histamine via histamine dehydrogenase and ferricenium, as mediator. In figure 22 that as the concentration of histamine increases there is practically no cathodic peak indicating the all the ferricenium generated is used up with the result that there is none to be reduced (the red curve is an example). It is important to emphasize that reaching a limiting current on a dose-response curve may be due to the limiting enzyme catalytic rate, the available ferricenium, or DET through the protein. In this case it is important to remember it will always be necessary to electrochemically generate the electron acceptor, ferricenium.

This reaction could be described by the following mechanism: In the presence of histamine and enzyme HDH, histamine is oxidized to imidazole acetaldehyde and the HDR (ox) is converted to HDR (red). The resulting reduced form of the enzyme HDH (red) is then reoxidized by the ferricenium ion, yielding ferrocene, which in turn is reoxidized at the underlying electrode with generation of an amperometric catalytic anodic current (Scheme 4).

Figure 22 - Cyclic Voltammetry to studies in solution, FcDM$^+$ 0.1 mM, Histamine dehydrogenase 1.5 μM and Histamine 0 (●), 0.025 (●), 0.25 (●), 0.300 (●) and 0.35 μM (●); 20 mV s^{-1}. Phosphate Buffer pH 7.4.
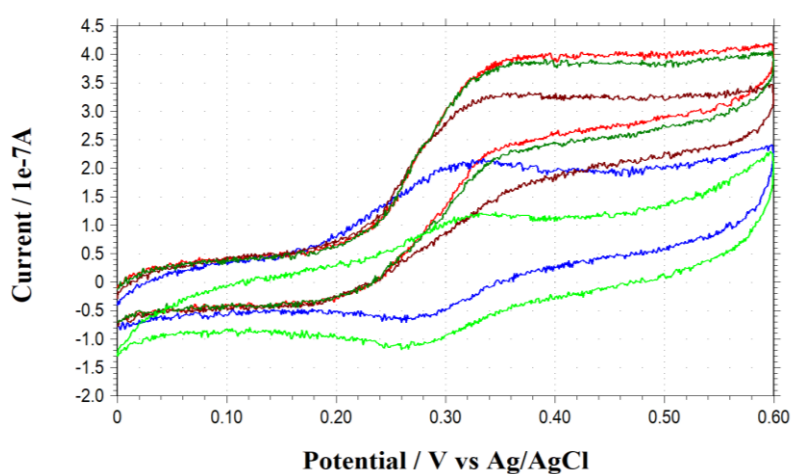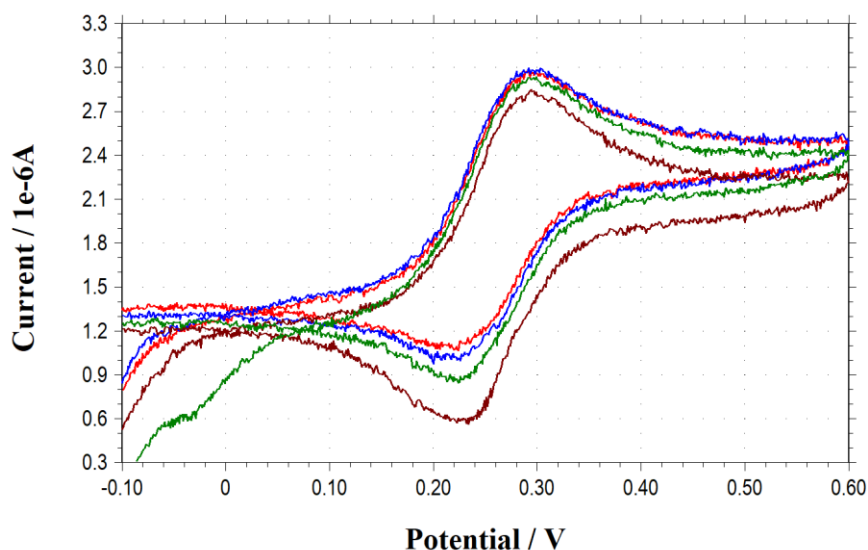

Source: Author, 2019

Scheme 4 - Steps in the catalytic electro-oxidation of histamine to imidazole acetaldehyde in the presence of histamine dehydrogenase (HDH) and an FcDM$^+$
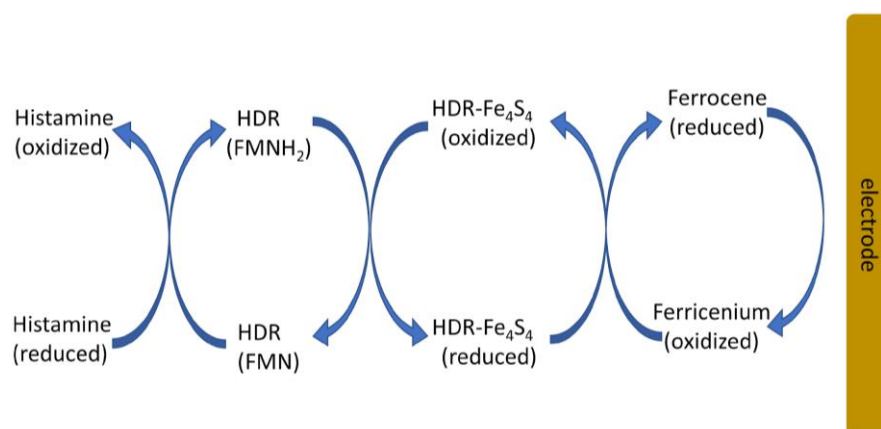
Source: Author, 2019

Similar profile was found when the enzyme was immobilized on the gold electrode surface but the catalytic behavior was less intense, CT-cAuBP-HDR (Figure 23) and WT-HDR (Figure 24). In mediated electrochemistry (MET), and following an EC′ mechanism, consumption of the redox mediator, i.e. the co-substrate, because of the catalytic reaction, is detected as a current amplification. This current increase is directly related to the amount of substrate being processed (SILVEIRA; ALMEIDA; 2013).

Figure 23 - Cyclic Voltammetry at gold electrode modified with ct-cAuBP-HDH (10µL/10µM dropped on the surface of the electrode and dried off), FcDM$^+$ 0.5 mM (●) and Histamine 0.25 (●), 0.45 (●), 0.65 mM (●). 20 mV s^{-1}. Phosphate Buffer pH 7.4.

Source: Author, 2019

Figure 24 - Cyclic Voltammetry at gold electrode modified with wild type-HDH (10µL/10µM dropped on the surface of the electrode and dried off), FcDM⁺ 0.5 mM (●) and Histamine 0.25 (●), 0.45 (●), 0.65 mM (●), 20 mV s⁻¹. Phosphate Buffer pH 7.4

.
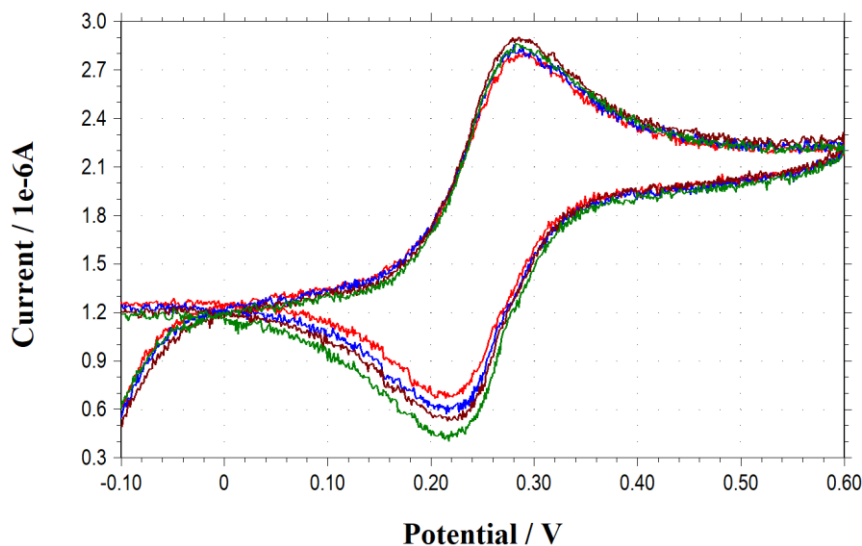
Source: Author, 2019

However, it is not uncommon to find monohemic cytochromes (Cyt) and other small proteins as a source or a sink of electrons in mediated electrochemical systems, and those were our first choice, but due to the slow rates showed previously in the section 4.2, Figure 13. Likewise, cytochrome C was exploited as mediator by cyclic voltammetry assay and there was no catalytic response even changing the immobilization process of that cytochrome or in solution (Figure 25) this cytochrome has a redox and reversible peak around -0.05 V. In fact, besides the use of physiological electron donors and/or acceptors to mimic more faithfully the charge transfer processes that occur in vivo, and thereby study intermolecular ET and enzyme kinetics, the enzyme– mediator protein coupling can be exploited in bioelectroanalytical applications. For the application of cytochrome C-HDR as second generation enzyme sensor constituent, mediator preference should be investigated and altered as it was achieved in an engineered fungus derived FAD-dependent glucose dehydrogenase (fFADGDH) with acquired ability to utilize hexaammineruthenium(III) as an electron acceptor by introducing mutation (OKURITA et al, 2018; OKUDA-SHIMAZAKI; YOSHIDA, SODE et al 2020)

Figure 25 - Cyclic Voltammetry of gold electrode modified with Cytochome C, Histamine 50 to 300 µM and HDH 2 µM. 50 mV s^{-1}. Phosphate Buffer pH 7.4.
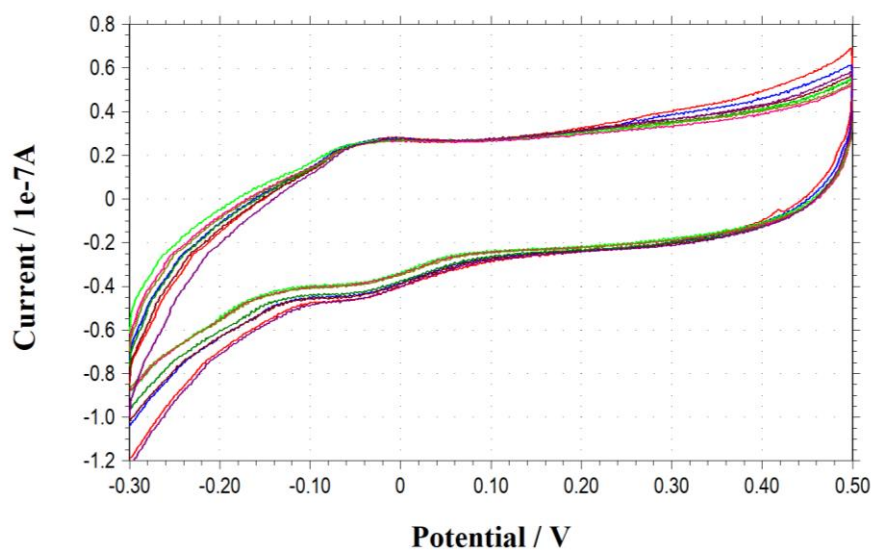
Source: Author, 2019

4.5.2 Amperometric studies

The dependence of response on applied potential was investigated at 400 mV when the histamine dehydrogenase *Rhizobium sp.* 4-9 and FcDM$^+$ were in solution to investigate them as a redox couple suitable for measuring histamine concentrations in biological samples. Figure 26 shows the typical current–time responses at gold bare electrode for successive addition of histamine. A significant rate of electron transfer was observed between histamine and a gold electrode when mediated by HDR and ferriceniumdimethanol at the range the histamine level in the brain (0.2 to 2 µM).

Figure 26 - (A) Amperometric results to studies in solution using Rotation Disc Electrode, (B) Plot of current versus histamine concentration. FcDM⁺ 2.5 mM, Histamine dehydrogenase 1 µM and Histamine 1 to 50 µM; 400 mV Phosphate Buffer pH 7.4.

A

B
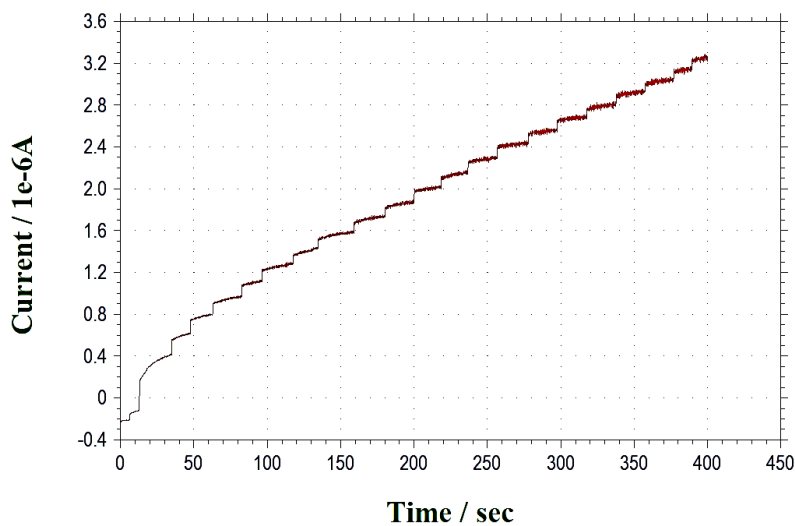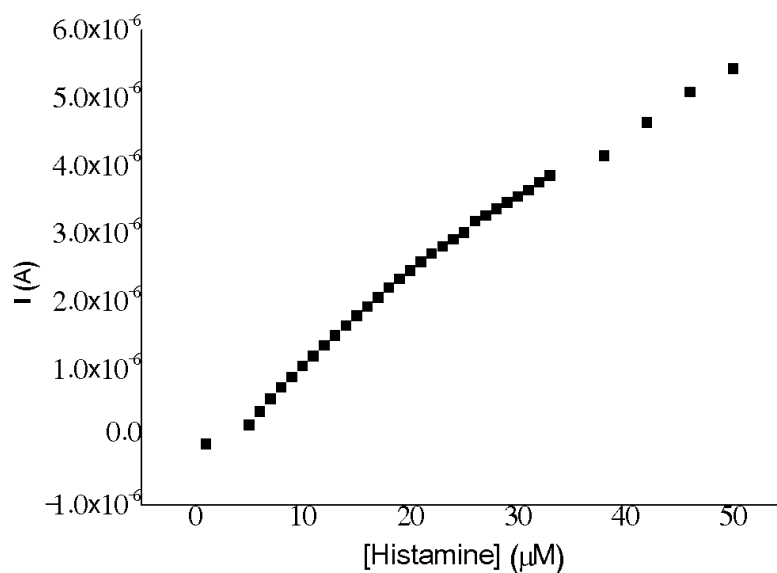
Source: Author, 2019

The current response of purified C- terminus cAuBP-HDH and wild-type enzyme was investigated after an aliquot of 10 µM was dropped on the electrode and let dry

for 2h, after that the electrode was washed off with buffer to remove adsorbed non-specific bind enzyme, Figure 27-A and B respectively. As shown, there is a linear response at the range of 0 to 50 µM as well the enzyme in solution, thus the immobilization approach did not interfere in the range of interest of our analysis and also show current response at concentrations as higher as 400 µM where it is seen a steady state of the assay.

Figure 27 - Amperometric response and plot of current versus histamine concentration for successive injection of Histamine (0-525 µM) at gold rotating disc electrode modified with ct-cAuBP-HDH (A) and WT-HDR (B)10 µM dropped on the electrode surface and wash off with buffer after 2h incubation); (FcDM$^+$) 1mM; 400 mV, 500 rpm, Phosphate buffer, pH = 7.4.

A

B
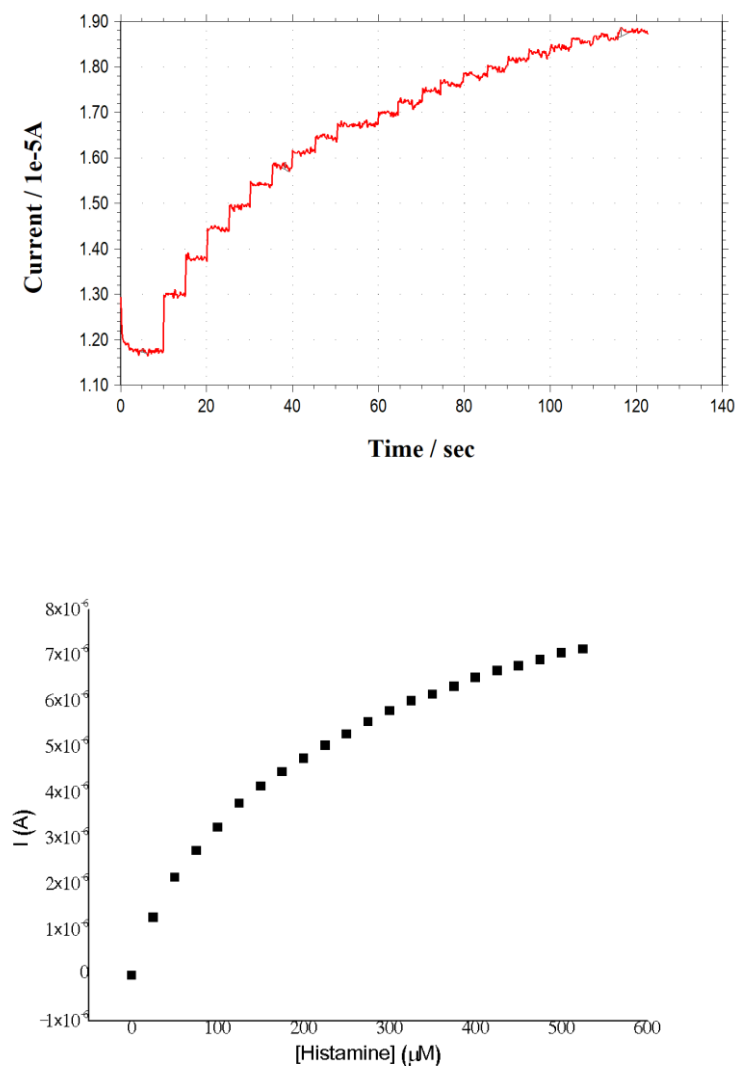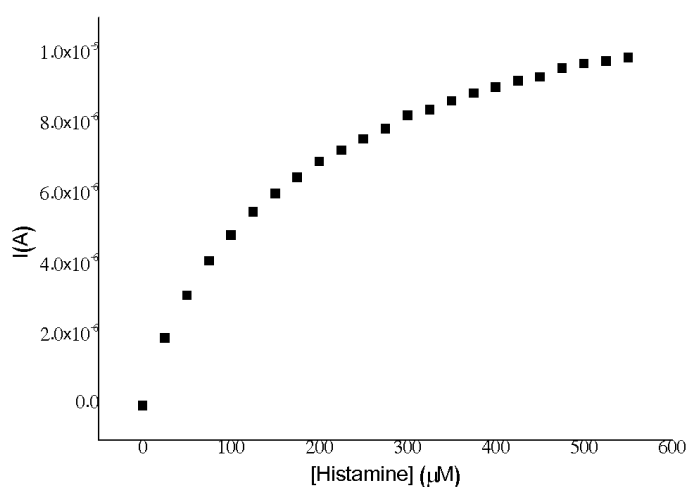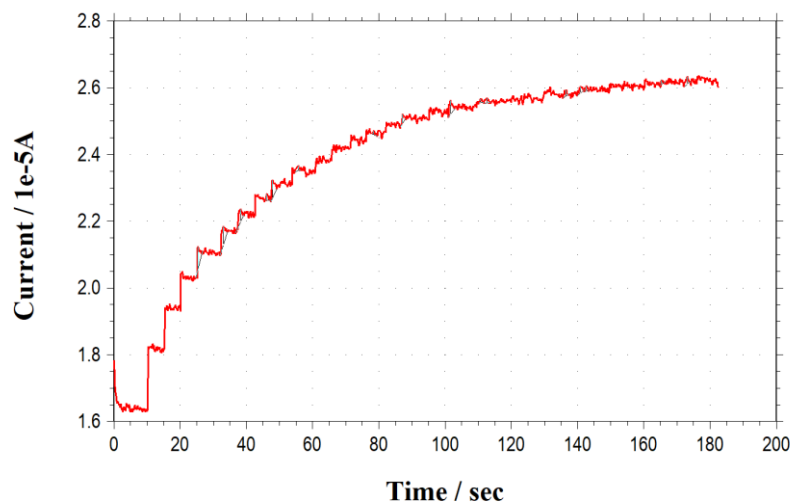
Different approaches were performed to maintain the activity and minimize the non-specific bind as shown in the previous sections of this report and it is the major issue when studying the self-assembly of the fusion protein on gold templates. Then, a wide-ranging the concentration of the C terminus fusion-enzyme was initially tested (1 to 10 µM) when it is dropped on the electrode surface and washed off several times with buffer after 2h. Figure 28 A-D shows the current response for successive histamine additions and a linear response is observed at different amounts of enzyme. When the current values are corrected and the plot current vs histamine concentrations

is obtained (Figure 29-A) a slightly different is observed, therefore there is no difference for the amperometric response at this enzyme concentration range. The same enzyme-modified electrode was tested at the same histamine concentrations after 3h of the first assay, the Figure 29-B shows the curves obtained for all the tested enzyme's concentration. The individual response curve can be seen in Figure 30, after 3h there was a decrease in the current response in all the concentrations, especially in higher concentration, these findings still suggest that there is a huge non-specific bind resulting in a loss of adsorbed enzyme between each analysis.

Figure 28 - Amperometric response for successive injection of Histamine at gold rotating disc electrode modified with 100µL of ct-cAuBP-HDH (A) 1µM, (B) 2 µM (C) 5µM, (D) 10µM dropped on the electrode surface and wash off with buffer after 2h incubation; FcDM+ 0.5, 400 mV. Phosphate Buffer pH 7.4.

A

B

C

D
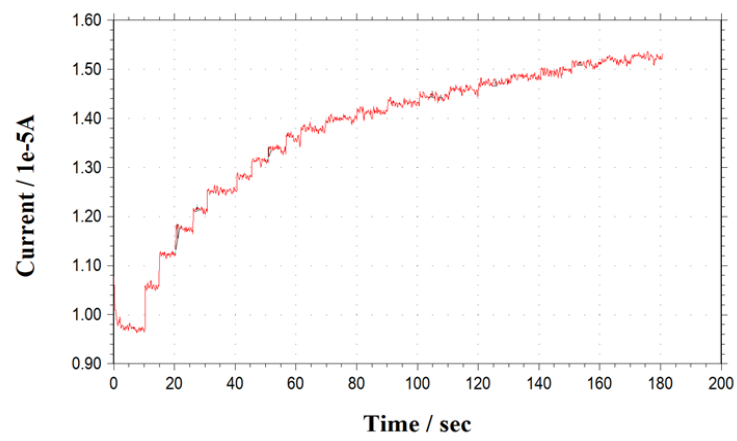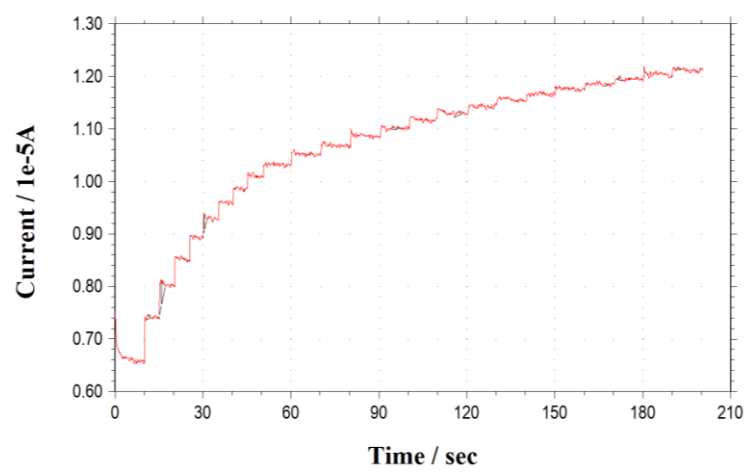
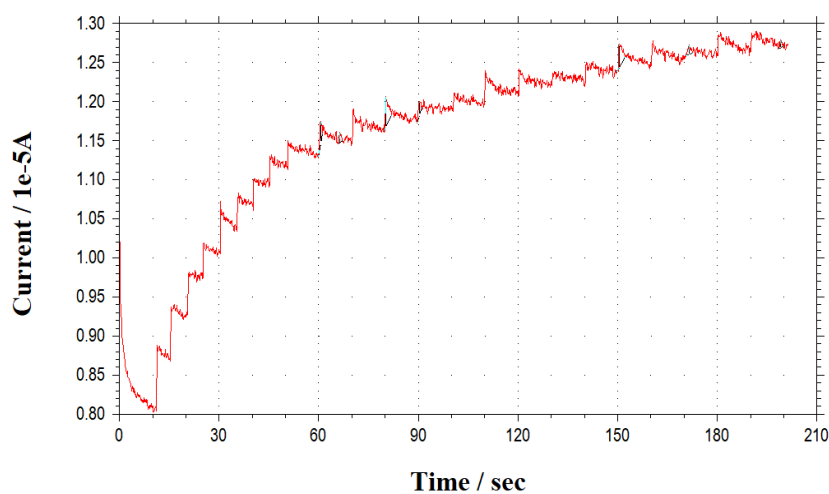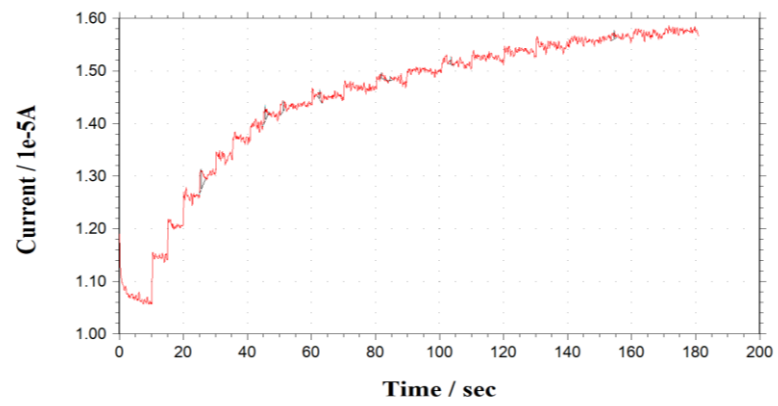Source: Author, 2019

Figure 29 - Plot of all responses obtained with ct-cAuBP-HDH (1μM, 2 μM, 5μM, 10μM) modified electrode (current x histamine concentration), initially and after 3h
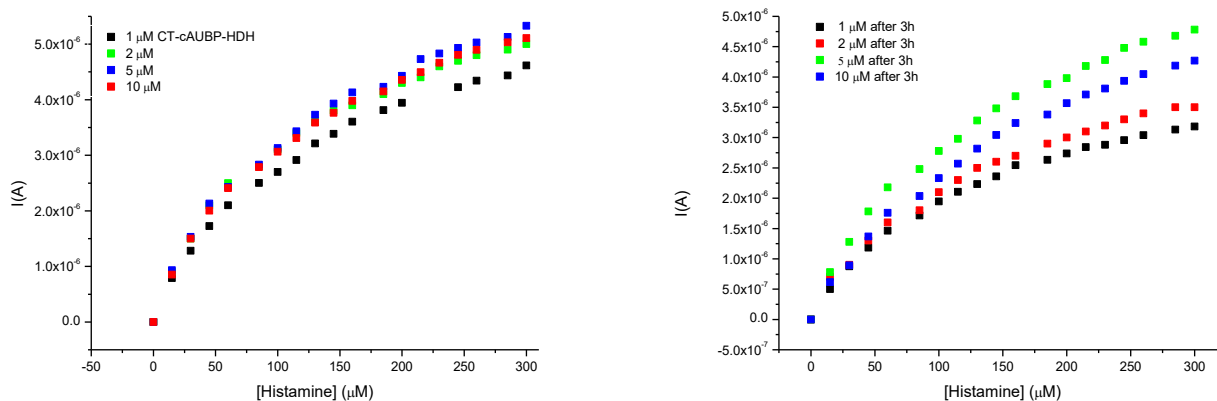
Source: Author, 2019

Figure 30 - Plot of current x concentrations of ct-cAuBP-HDH (A) 1μM, (B) 2 μM (C) 5μM, (D) 10 μM dropped on the electrode surface and wash off with buffer after 2h incubation.

A

B

C

D
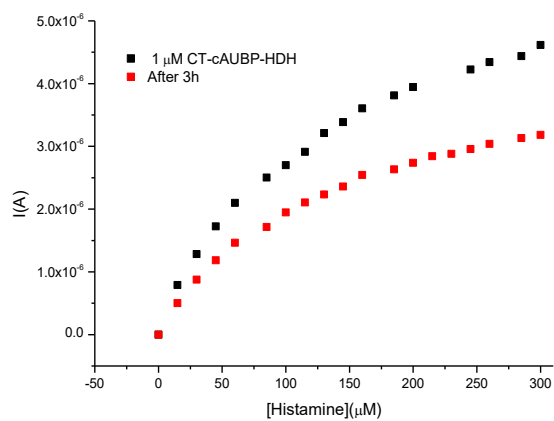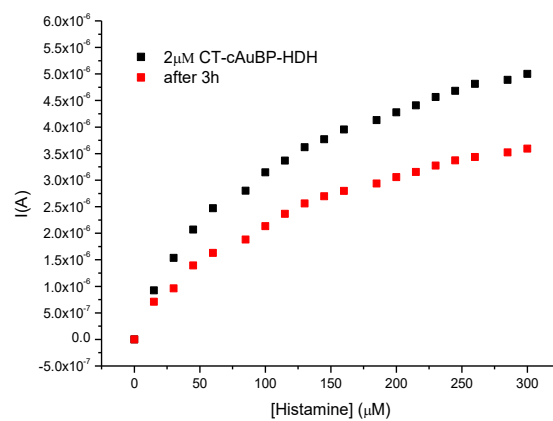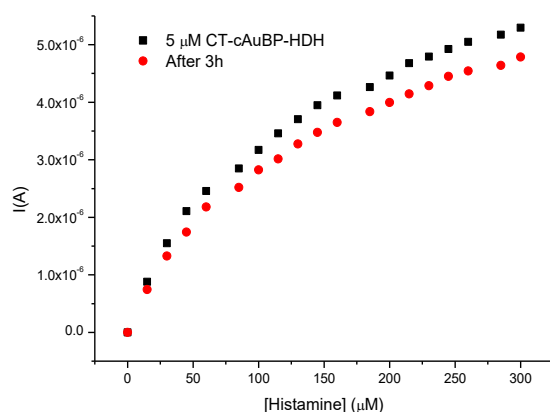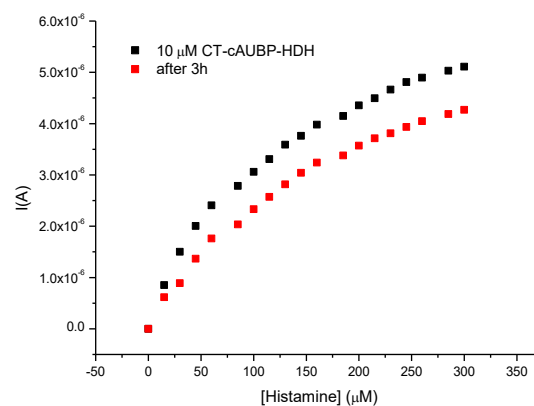
Source: Author, 2019

Since there was no significant change between the enzyme concentration range studied, a lower amount of enzyme was tested (0.5µM) for both wild-type and CT-cAuBP-HDR (Figure 31) and a good current-response is observed in each case. Furthermore, the current response was obtained after 3h and 24h and as well as higher concentrations there was a decrease in the current values, but less intense in the range 0 to 50 µM of histamine (Figure 31 A-B) and best seen in the Figure 32 which was of a loss of 55.5% to the CT-cAuBP-HDR and 52.8% to the wild type, so even the response is slightly higher to the fusion enzyme, as seen before the wild-type also binds strongly to gold surfaces and retain enzymatic activity similar to that genetically modified with a well-defined and studied gold binding-peptide.

Figure 31 - Amperometric response for successive injection of Histamine (0 to 300 μM) at gold rotating disc electrode modified with 100μL of CT-cAuBP-HDH (A) 0.5 and WT-HDH (B) 0.5 μM dropped on the electrode surface and wash off with buffer after 1h incubation; FcDM$^+$ 1 mM; 400 mV. Phosphate Buffer pH 7.4.

A

B
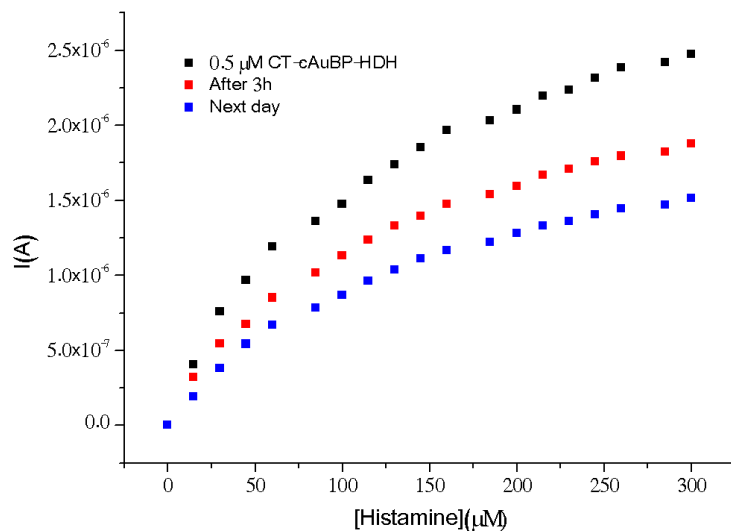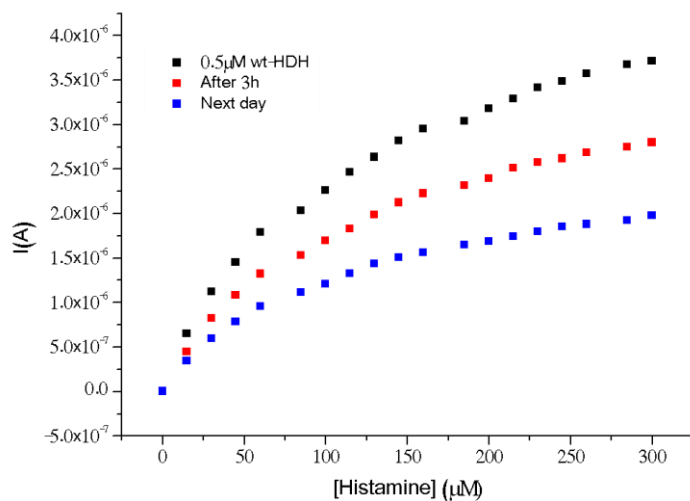
Source: Author, 2019

Figure 32: Amperometric response for successive injection of Histamine (0 to 145 µM) at gold rotating disc electrode modified with 100µL of CT-cAuBP-HDH (A) 0.5 and WT-HDH (B) 0.5 µM dropped on the electrode surface and wash off with buffer after 1h incubation; FcDM$^+$ 1 mM; 400 mV. Phosphate Buffer pH 7.4.

A

B
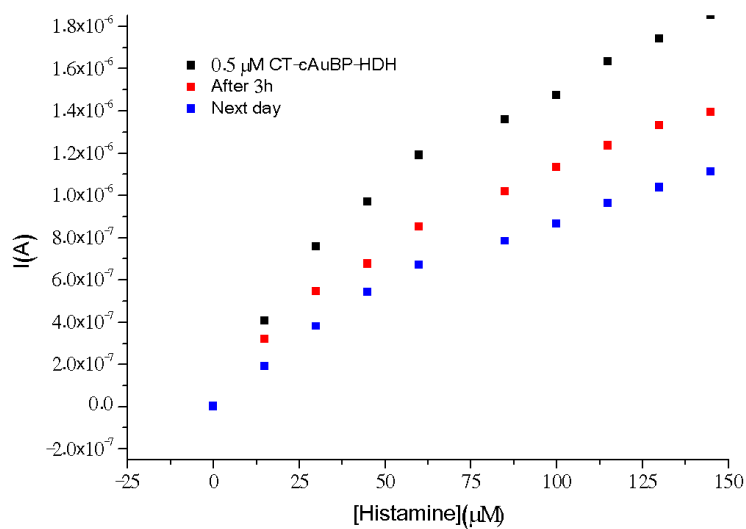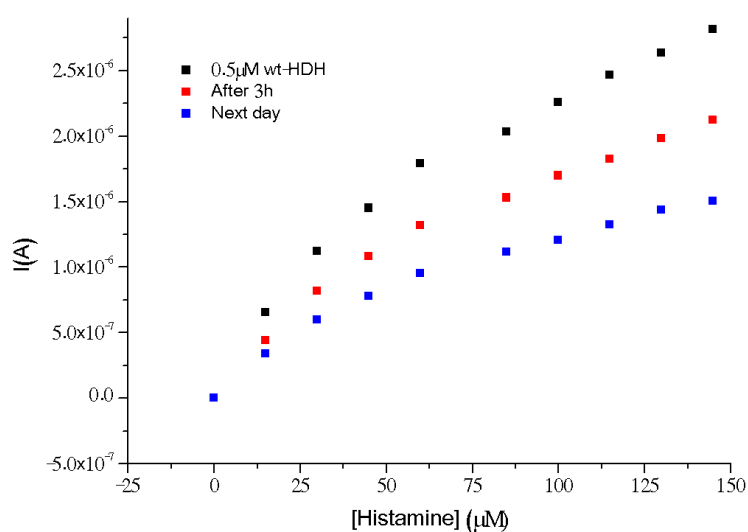
Source: Author, 2019

In addition to the concentration evaluation that was carried out, it was tested if the enzyme could have responded after being dried off using a flow of an inert gas as N$_2$ and immobilization time or maintaining the washing with buffer several times (Figure 33 and 34) and as expected washing, several times minimize the non-specific bind that is already higher to the histamine dehydrogenase. The difference of the current response at different ferricenium concentration was performed in the Figure 35-A and no significant difference was observed when the concentration is 0.5 or 1 mM, however huge difference was found when the immobilized enzyme was desalted 7 days before the experiment figure 35-B, for that reason all the previous assays were carried out with fresh enzyme

Figure 33 - Amperometric response for successive injection of Histamine at gold electrode modified with A) CT-cAuBP-HDH and B) WT-HDH (100µL/10µM) dropped on the electrode surface and dried off with N$_2$ after 2h); FcDM+ 1 mM; 400 mV s. Phosphate buffer pH 7.4

A

B

Source: Author, 2019

Figure 34 - Amperometric response for successive injection of Histamine at gold electrode modified with A) CT-cAuBP-HDH and B) WT-HDH (100µL/10µM) dropped on the electrode surface and washed off with buffer after 2h); FcDM$^+$ 1 mM; 400 mV s. Phosphate buffer pH 7.4

Source: Author, 2019

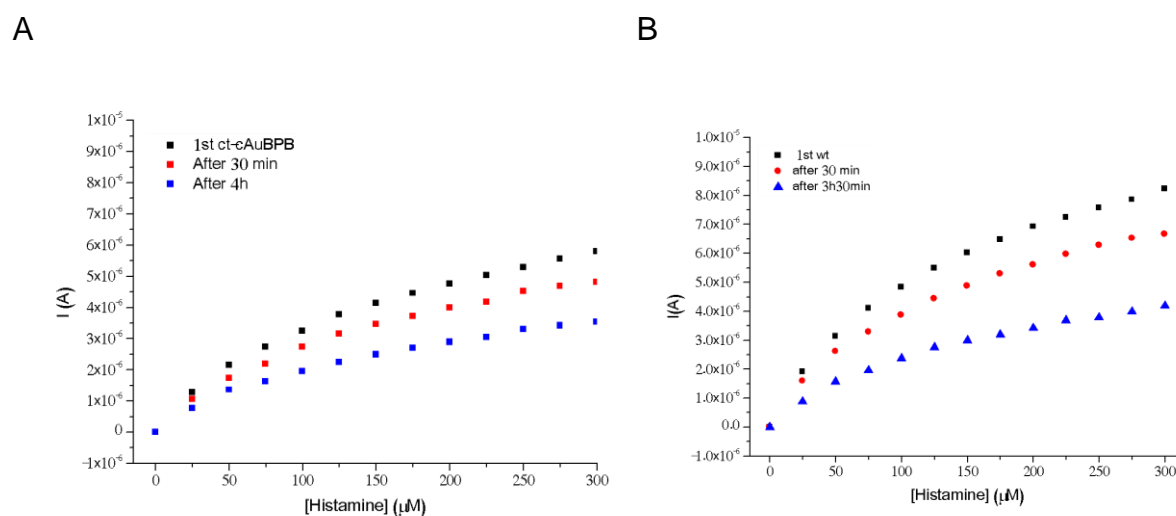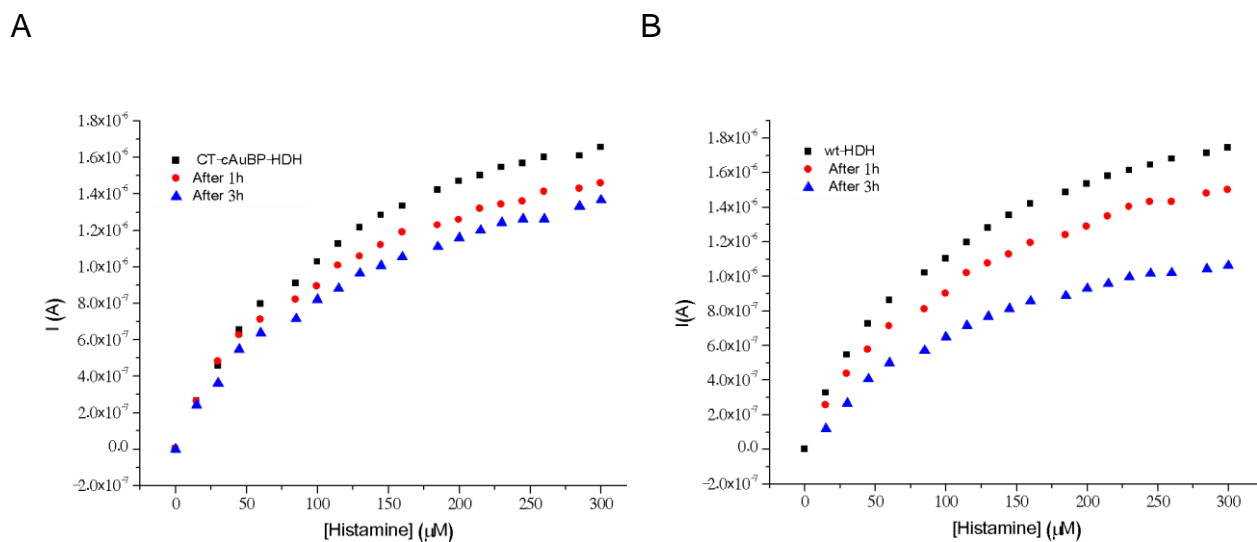**Figure 35** - (A) The influence of FcDM+ concentration (•) 1mM and (•) 0.5 mM (B) The current values difference between fresh and 7 days old, desalted enzyme; 400 mV s. Phophate Buffer pH 7.4.

A

B
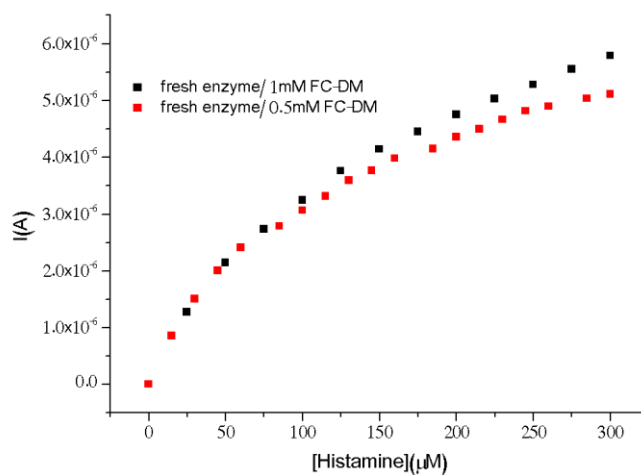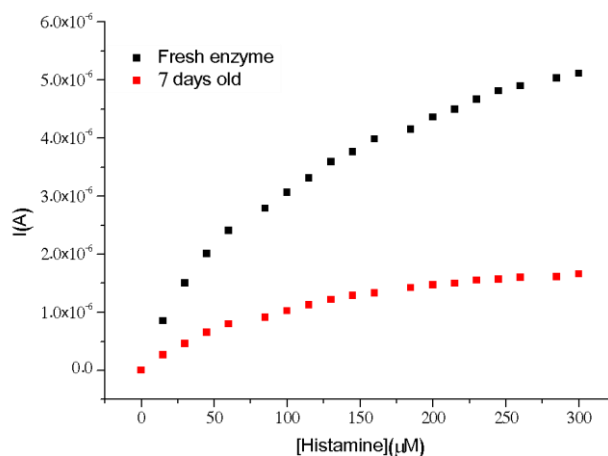
Source: Author, 2019

The gold binding peptide has also been used successfully in electrochemical biosensors with AuNP-anchored graphene sheets. Yang et al 2011 used organophosphorus hydrolase (OPH) as a model enzyme. Key to this particular model system is the chemically modified graphene, which contains the AuNPs, increasing the electroactive area and facilitating electron transfer, but also providing an ordered binding point for the GBP (fused with OPH). The GBP-OPH biosensor system was successfully demonstrated for the detection of paraoxon (2 to 20 mM). The use of nanoparticles was also employed in previous discussed report of the Lee and coworkers (2019) report that showed a significant enhancement of direct electric communication across enzyme-electrode when using gold nanoparticle (AuNP)-modified electrode. Therefore, the AuNP can be an alternative to increase the specific and controlled bind of the enzyme on electrode, and maybe the DET can be achieved, which will also enable a good sensitive and stable biosensor.

Developing a biosensor based on flavin dehydrogenase enzymes presents several issues that must be addressed. Usually, a second electroactive component is needed, such as a derivative ferrocene, to shuttle electrons from the reduced flavin/iron sulfur center of the enzyme to the electrode surface. This can be achieved by coating a redox dye onto the electrode surface or by coupling the HDR to small redox proteins such as cytochromes but none of these methods have proven adequately efficient for *in vivo* sensor development. Thus, to overcome this problem we are suggesting a new approach to obtain the histamine biosensor by covalently

attaching a small redox mediator (Ferrocene) to the enzyme using a peptide linker terminated with a reactive moiety. Martic and coworkers (2011) have been shown that a ferrocene derivative with attached poly-amino acid and polyethylene glycol chain retain their electron transfer capability indicating the feasibility of this approach.

4.6 Investigation of the non-specific biding

Given the binding results found so far, and the similarities between the profile presented in both wild type and the enzyme with gold-binding peptide we decided to investigate it, and we supposed that Histidine tag within our design, and used for the rapid purification of the protein, contributes to the binding of the WT-HDR proteins to gold surface. Several studies show that histidine tags are known to bind to gold substrate (Peelle et al., 2005; Presnova et al., 2000; Slocik and Wright, 2003). Then, to avoid further nonspecific interactions of the histidine-tag with the gold surface and limit binding only to the gold-binding peptide, we removed the His-tag region from the enzyme and confirmed that apparent kinetic parameters were not affected. Also, investigating residues that might participate to the non-specific binding on gold surfaces, the surface exposed cysteine (Cys601) on the protein was also thought to be a potential contributor to binding and this residue has been mutated to Serine (HDR-C601S) and the enzyme with gold peptide as well (cAuBP-HDR-C601S) and the studies using the mutant enzymes has been performed.

Spectral and electrochemical data was collected to evaluate the enzymatic activity after the removal of the his-tag, using $FcDM^+$, as the mediator (Fig. 36 and 37), and all the studies were done in solution. The kinetics data obtained through spectrophotometry show that cAuBP-HDR-C601S protein has faster rate than the HDR-C601S and the wt-HDR (Table 7). Electrochemistry experiments were performed in solution using Rotating Disc electrode (RDE), the kinetics data from this experiment suggested that the protein with gold binding tag has activity somewhere in between the wt-HDR and the HDR-C601S (Table 8). The results suggest that the removal of the histine tag does not interfere with the enzyme function, and it can improve that activity.

Figure 36 - Spectral Data using 0.25µM protein (●) HDR-C601S (wo his-tag), (●) CT-cAuBP-HDR-C601S, (●) wt-HDR (wo his-tag), 2.5mM FcDM$^+$ and 0.1M KH2PO4 buffer, pH=7.4.
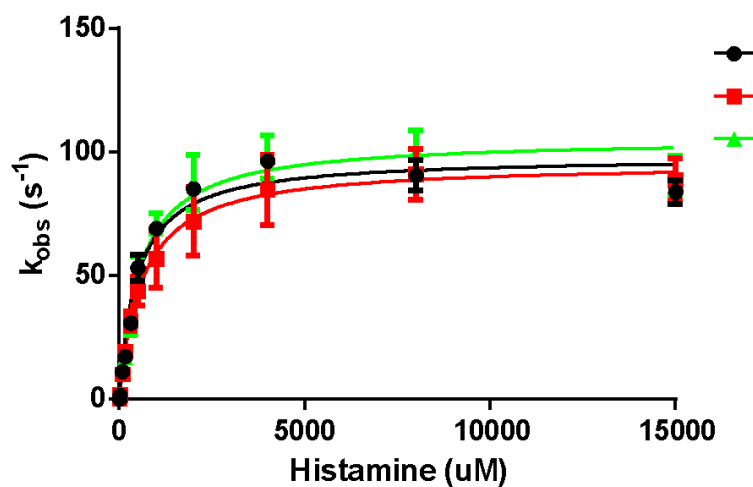
Author: 2020

Table 7 - Kinetic parameter for the wild-type HDH, the mutant HDH-C601S and cAuBP-HDH-C601S, all without the histidine tag obtained through spectrophotometry.

	HDH-wt (wo_His)	**HDH-C601S** (wo_His)	**cAuBP-HDH-C601S** (wo_His)
V$_{max}$	98.15	95.51	105.5
K$_m$	481.1	611.6	555.8

Author: 2020

Figure 37 - Electrochemistry studies in solution using 0.25uM protein, (●) HDR-C601S (wo his-tag), (●) CT-cAuBP-HDR-C601S, (●) wt-HDR (wo his-tag). 2.5mM FcDM⁺ and 0.1M KH2PO4 buffer, pH=7.4.
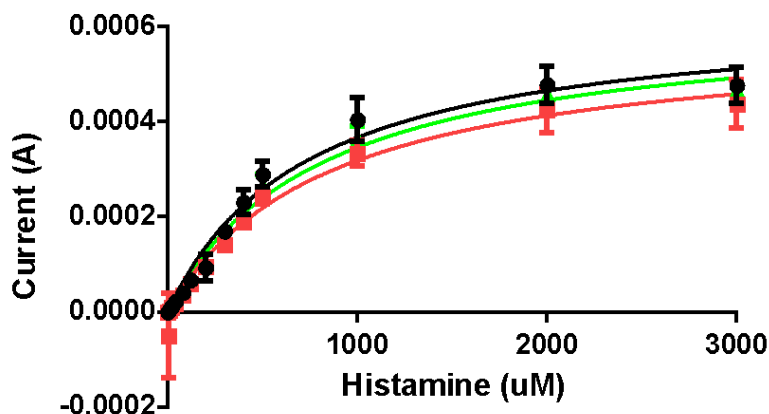
Table 8 - Kinetic parameter for the wild-type HDH, the mutant HDH-C601S and cAuBP-HDH-C601S, all without the histidine tag obtained through electrochemistry

	HDR-wt (wo_His tag)	**HDR-C601S** (wo_His tag)	**cAuBP-HDH-C601S** (wo_His tag)
Vmax	0.0006354	0.0005866	0.0006242
Km	730.8	841.0	804.3

Author: 2020

4.7 SPR Studies

SPR spectroscopy was used to check the gold-binding ability of CT-cAuBP-HDH and WT-HDH enzymes. This ability was analyzed at different buffers and protein concentrations. These studies allow for investigation of the kinetics of binding and the adsorption and desorption rates. This would mean that a lot of the protein adsorbs to the surface and only a small amount of adsorbed protein is easily removed. SPR can be used to indirectly check the orientation of the protein in future studies. Additionally, this technique allows for the determination of interaction specificity with hopefully only a little nonspecific adsorption occurring, another key goal of these studies.

Initially, the wild type with and without his-tag (wo his-tag) and the mutation HDR-C601S were investigated to see the binding difference between them as it is showed in the Figure 38. A gold chip was utilized for this experimental portion where it

a chip was docked into the SPR machine. As the protein was injected, the SPR response increased, due to a change in refractive index to the surface. As more protein was introduced to the surface, the initial curve increases as protein adsorbed from solution. The magnitude of this response is indicative of the amount of protein bound to the surface; the higher the response, the more protein that was bound to the surface. Additionally, a reference cell was run in parallel to eliminate the difference in refractive index between the buffer and the sample.

From these results, it was decided that to avoid confusion in the following experiments will be used HDR-C601S without his-tag as the new wildtype and CT-cAuBP-HDR-C601S as our protein with the gold tag at C-Terminus

Figure 38 - SPR spectroscopy results of (●) wt-HDR (his-tag) (●) wt-HDR (wo his-tag) (●) HDR-C601S binding to gold surfaces at 1 μM concentration. (10 mM Tris-Cl, pH=7.5, 1μM)
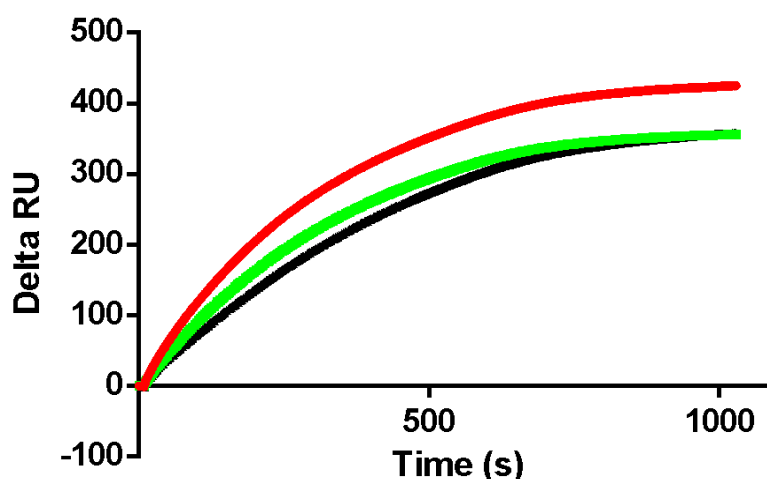
Author: 2020

Prior to carrying out the following studies, it was essential to identify the optimum buffer conditions for the efficient and maximal immobilization of the CT-cAuBP-HDR. To identify these conditions, the substrate protein (1 μM) was diluted in sodium phosphate buffer and TRIS-Cl with pH 7.4 and 7.5, respectively (Figure 39 and 40). These buffers were then injected over the sensor surface and the signal (RU) noted. The buffer, concentration and conditions that gives the highest signal for CT-cAuBP-HDR is what we were looking for further studies. It was observed that sodium phosphate buffer pH 7.4 (20mM) gave the highest immobilization signals to HDR-

C601S than to CT-cAuBP-HDH attaching onto the sensor surface yielding a signal of about over 1000 RU.

The wild-type enzyme was exhibiting greater binding than expected (Figure 39) in phosphate buffer but about the same in TRIS-Cl buffer pH 7.5 (10 mM) yielding a signal of about 350 RU. Ideally, the gold-peptide enzyme would have higher signal the wild type however in the previous binding studies in this work we found similar results where we see strong nonspecific protein binding to the gold surface, even after the histine tag removal. Unlike other physical techniques utilized previously in this work that required us to measure protein quantities at specific time points, SPR reports the real-time binding of molecules. SPR is an extremely powerful and facile method of studying interaction kinetics.

Figure 39 - SPR spectroscopy results of HDR-C601S (●) and CT-cAuBP-HDR (●) binding to gold surfaces at 1 µM concentration. (20 mM sodium phosphate buffer, pH = 7.4)
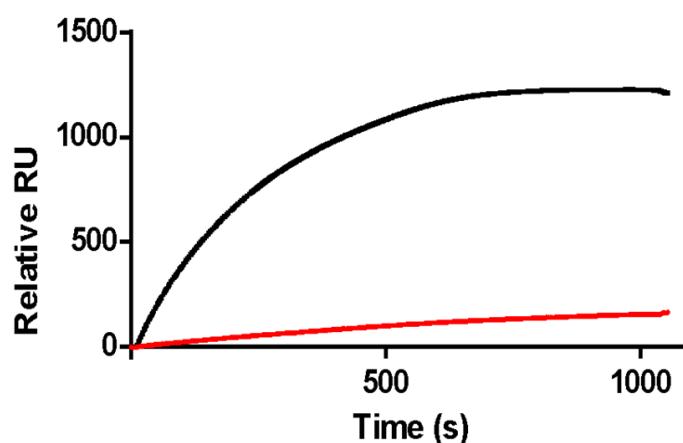
Author: 2021

Figure 40 - SPR spectroscopy results of (●) HDR-C601S and (●) CT-cAuBP-HDR binding to gold surfaces at 1 μM concentration. (10 mM Tris-Cl, pH=7.5)
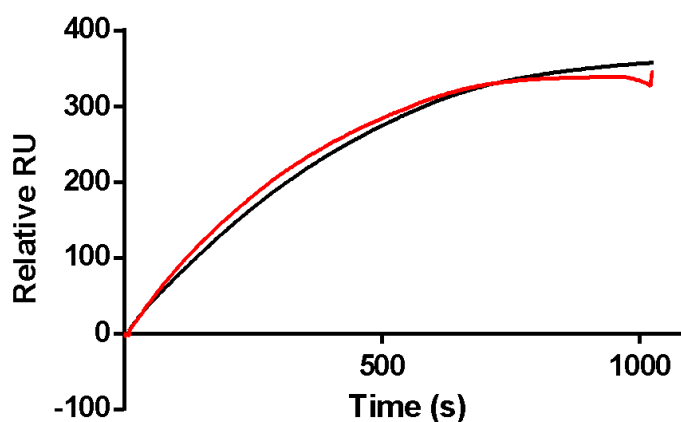
Author: 2021

The effect of salts added to these buffers were also investigated at the same time titrations at different concentrations of the enzymes were performed (0.1μM- 10 μM) to see how the binding curve looks. All measurements were collected under identical conditions, making the results directly comparable. After a stable baseline signal was established by allowing 10 mM of TRIS-Cl buffer (pH 7.5) to flow over the Au surface, solutions of the wild type or genetically engineered proteins were allowed to flow over the surface. The amount of enzyme immobilized on the Au surface increased over time until it reached a steady state, at which point the surface coverage was in equilibrium with the enzyme concentration in the solution. This interaction was concentration dependent as expected. The higher the concentration, the more protein adsorbed to the surface, although around 7 μM we see an atypical behavior CT-cAuBP-HDR.

Figure 41 - SPR spectroscopy results obtained from 0.1 to 10 µM of the (●) HDR-C601S and (●) CT-cAuBP-HDR to bare gold surfaces in 10 mM of TRIS-Cl buffer (pH 7.5)
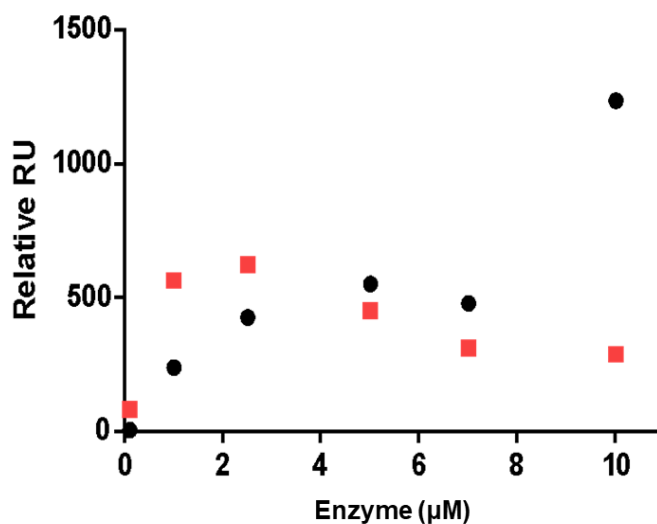
Author: 2021

Figure 42 - SPR spectroscopy results obtained from 0.1 to 10 µM of the (●) HDR-C601S and (●) CT-cAuBP-HDR to bare gold surfaces in 10 mM of TRIS-Cl buffer (pH 7.5) + 100 mM NaCl
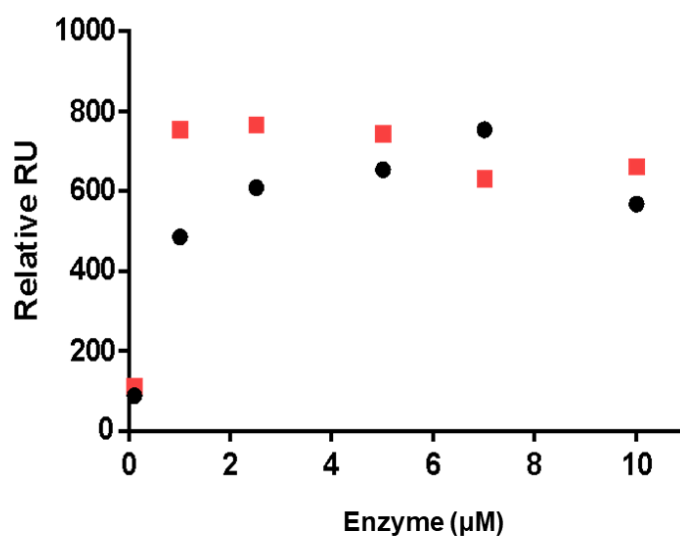
Author: 2021

Figure 43 - SPR spectroscopy results obtained from 0.1 to 10 µM of the (●) HDR-C601S and (●) CT-cAuBP-HDR to bare gold surfaces in 20 mM of NaPO4 buffer (pH 7.4)
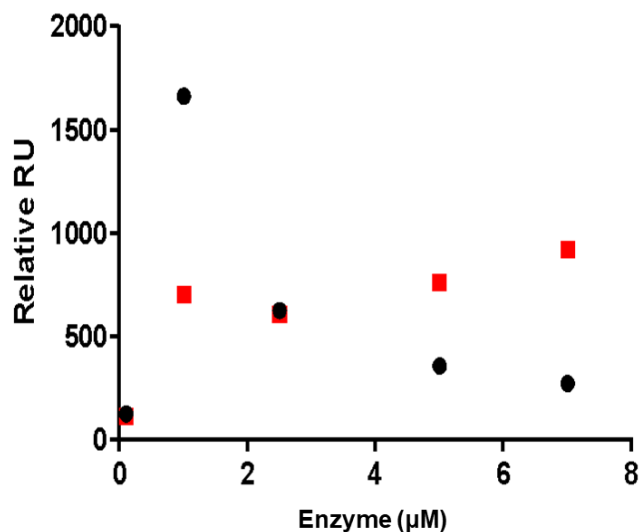
Author: 2021

An experiment at a fixed concentration (0.5 µM) was done to see how the two proteins interact with the surface using 10mM Tris-Cl, pH=7.5 buffer. The result show that the HDR-C601S is still binding better than the HDR-C601S-CT-cAuBP tag using 10mM Tris-Cl, pH=7.5 buffer. The experiments at a concentration (0.5 µM or 1µM) using 10mM Tris-Cl, pH=7.5 and 100 mM NaCl could not be performed to date but It would be interesting to look closer the differences in binding between the HDR-C601S and HDR-C601S-cAuBP without His-tags proteins in this condition.

Titration studies showed that at lower concentrations HDR protein with gold tags bind better than the HDR wild type at least in the 10mM Tris-Cl, pH=7.5 and 10mM Tris-Cl, pH=7.5+100 mM NaCl. The SPR results along with the other binding studies performed in this work showed that the despite the similar intensity, the wild type and the genetically engineered enzyme presented different binding behaviors.

CONCLUSION

A genetically engineered histamine dehydrogenase from *Rhizobium* sp. 4-9 with a highly specific cyclic gold-binding peptide (cAuBP) was successfully expressed and kinetic and surface binding assays were performed. The Kinect assays showed that after the introduction of a new functionalized tag the enzyme retained its catalytic activity either on C-terminus or N-terminus. It was also possible to identify a good electron acceptor, the oxidized form of 1,1- ferrocenedimethanol, which provided the most robust turnover between other molecules tested.

Surface-binding kinetics data indicated that CT-cAuBP-HDR can adsorb onto gold surface at relatively low concentrations but so does the wild-type HDR. The main difference could be seen on the AFM analysis, where the CT-cAuBP-HDR presented an increment of 1.5 nm on its height. The SPR studies suggested that at lower concentrations and with Tris-Cl buffer (10mM + 100 mM NaCl, pH=7.5) the genetically engineered enzyme has a better bind onto gold surface. The retained CT-cAuBP-HDR activity on the surface proves that the fusion construct can deliver the enzyme function for preferable applications. Finally, the detection of the electrochemical reaction performed by immobilized enzyme suggested that HDR provides an efficient method for histamine.

Inorganic-binding peptides have been investigated as an alternative biofunctionalization method for a variety of material surfaces for addressable-oriented protein and/or enzyme immobilization using a single-step biofriendly procedure. However, additional studies have to be made for orientation and control of enzymes on the surfaces using inorganic-binding peptide tags. Each peptide and enzyme set needs to be evaluated in detail once they are genetically conjugated to achieve their individual optimal performance. Controlling the biological-materials interfaces, biofunctionalization of metallic or semiconductor surfaces has great potential in creating addressable and genetically programmable biomolecular templates that can contribute to the developments of the next generation of biosensors.

REFERENCES

BAKKE, M. et al. Histamine dehydrogenase from *Rhizobium sp.*: gene cloning, expression in *Escherichia coli*, characterization and application to histamine determination. *Journal of biotechnology,* 119.3, 2005, 260-271.

BINAY, B. Highly stable and reusable immobilized formate dehydrogenases: Promising biocatalysts for in situ regeneration of NADH. Beilstein. Journal of Organic Chemistry, 12, 2016, p 271-277.

BOLLELLA, P.; GORTON, L. "Enzyme based amperometric biosensors." *Current Opinion in Electrochemistry* 10 (2018): 157-173.

BOLLELLA, P.; GORTON, L.; ANTIOCHIA, R. "Direct electron transfer of dehydrogenases for development of 3rd generation biosensors and enzymatic fuel cells." *Sensors* 18.5 (2018): 1319.

BOYD, G., et al. Trimethylamine dehydrogenase ofbacteriumW3A1. FEBS Lett. 308, 271–276, 1992.

BRANCO, A. C. C. C. et al. Role of histamine in modulating the immune response and inflammation. *Mediators of inflammation.* 2018.

CACABELOS, R. et al. Histamine and immune biomarkers in CNS disorders. *Mediators of inflammation*, 2016.

CETINEL, S. et al. Addressable self-immobilization of lactate dehydrogenase across multiple length scales. *Biotechnology journal.* 8.2, 2013, 262-272.

CHANG, S-Y, et al. Wireless fast-scan cyclic voltammetry measurement of histamine using WINCS–a proof-of-principle study. *Analyst* 137.9, 2012, 2158-2165.

CHAZOT P., et al. Histamine receptors (version 2019.4) in the IUPHAR/BPS Guide to Pharmacology Database. *IUPHAR/BPS Guide to Pharmacology CITE, 2019(4).* Available on: https://www.guidetopharmacology.org/GRAC/ObjectDisplayForward?objectId=263

CONNELLY, W. M. et al. The histamine H4 receptor is functionally expressed on neurons in the mammalian CNS. Br. J. Pharmacol. 157, 2009. 55–63.

FERREIRA R.et al. Histamine modulates microglia function. J. Neuroinflamm. 9, 90. 2012.

FLIK, G. et al. "Interaction between brain histamine and serotonin, norepinephrine, and dopamine systems: in vivo microdialysis and electrophysiology study." *Journal of Molecular Neuroscience* 56.2, 2015, 320-328.

FUJIEDA, N. et al. 6-S-Cysteinyl flavin mononucleotide-containing histamine dehydrogenase from *Nocardioides simplex*: molecular cloning, sequencing, overexpression, and characterization of redox centers of enzyme. *Biochemistry,* 43.33, 2004, 10800-10808.

GAUVREAU, V. et al. Engineering surfaces for bioconjugation: developing strategies and quantifying the extent of the reactions. Bioconjugate chemistry, 15, 2004, 1146-1156

GOYAL, P. LOVELL, S. RICHTER, M. Crystal structure of Histamine desydrogenase from Rhizobium sp. 4-9, 2.1 A resolution. Available on: https://www.rcsb.org/structure/6DE6

GREWAL, J.; AHMAD, R.; KHARE, S. K., Development of cellulase-nanoconjugates with enhanced ionic liquid and thermal stability for in situ lignocellulose saccharification. Bioresource Technology, 242, 2017, 236-243.

GRIESHABER, D. et al. Electrochemical biosensors-sensor principles and architectures. *Sensors,* 8.3, 2008, 1400-1458.

HAAS, H. L., SERGEEVA, O. A., SELBACH, O. Histamine in the nervous system. *Physiological reviews*, *88*(3), 2008, 1183-1241.

HAAS, H. PANULA, P. The role of histamine and the tuberomamillary nucleus in the nervous system. *Nature Reviews Neuroscience* 4.2, 2003, 121-130.

HENAO-ESCOBAR, W., et al. Dual enzymatic biosensor for simultaneous amperometric determination of histamine and putrescine. *Food chemistry,* 190, 2016, 818-823.

HITAISHI, V. P. et al. Controlling redox enzyme orientation at planar electrodes. *Catalysts.* 8.5, 2018, 192.

HNILOVA, M. et al. Effect of molecular conformations on the adsorption behavior of gold-binding peptides. *Langmuir.* 24.21, 2008, 12440-12445.

HUTH, J.R., et al. Design of an expression system for detecting folded protein domains and mapping macromolecular interactions by NMR. Protein Sci 6:2359–2364, 1997.

KACAR, T., et al. "Directed self-immobilization of alkaline phosphatase on micro-patterned substrates via genetically fused metal-binding peptide." *Biotechnology and bioengineering* 103.4 (2009): 696-705.

Kamathewatta, N.J.B., et al. "Self-immobilized putrescine oxidase biocatalyst system engineered with a metal binding peptide." Langmuir 36.40 (2020): 11908-11917.

KEHR, J. YOSHITAKE.T. Determination of histamine in microdialysis samples from the rodent brain by column liquid chromatography." *Microdialysis Techniques in Neuroscience*. Humana Press, Totowa, NJ, 2013. 299-320.

KRAULAND, E. M. Peptide tags for enhanced cellular and protein adhesion to single-crystalline sapphire. Biotechnology and bioengineering, 97, 2007, 1009-1020.

LEE, H., et al. "Significant enhancement of direct electric communication across enzyme-electrode interface via nano-patterning of synthetic glucose dehydrogenase

on spatially tunable gold nanoparticle (AuNP)-modified electrode." *Biosensors and Bioelectronics* 126 (2019): 170-177.

LEE, Y. S. et al. Construction of Uniform Monolayer-and Orientation-Tunable Enzyme Electrode by a Synthetic Glucose Dehydrogenase without Electron-Transfer Subunit via Optimized Site-Specific Gold-Binding Peptide Capable of Direct Electron Transfer. *ACS applied materials & interfaces* 10.34, 2018, 28615-28626.

LEURS R. et al. Molecular and biochemical pharmacology of the histamine H4 receptor. Br. J. Pharmacol. 157, 2009. 14–23.

LOPEZ MS, REDONDO-GOMEZ E, LOPEZ-RUIZ B. Electrochemical enzyme biosensors based on calcium phosphate materials for tyramine detection in food samples. Talanta. 2017; 175:209–216.

LUONG, J. H. et al. *U.S. Patent No. 5,432,274.* Washington, DC: U.S. Patent and Trademark Office, 1995.

LUPPA, P. B.; SOKOLL, L. J.; CHAN, D. W. Immunosensors - principles and applications to clinical chemistry. Clinica Chimica Acta, 314(1-2), 2001.

MARTIC, S., et al. "Use of 5′-γ-ferrocenyl adenosine triphosphate (Fc-ATP) bioconjugates having poly (ethylene glycol) spacers in kinase-catalyzed phosphorylations." *Bioconjugate chemistry* 22.8 (2011): 1663-1672.

MICHAEL, A. C., BORLAND, L. *Electrochemical methods for neuroscience.* CRC press, 2006.

NAIK, R. R. Biomimetic synthesis and patterning of silver nanoparticles. Nature materials, 1, 2002, 169-172.

NGUYEN, H. H. et al. "Immobilized enzymes in biosensor applications." *Materials* 12.1 (2019): 121.

OKUDA-SHIMAZAKI, J.; YOSHIDA, H.; SODE, K. "FAD dependent glucose dehydrogenases–discovery and engineering of representative glucose sensing enzymes." *Bioelectrochemistry* (2019): 107414.

OKURITA, M., et al. "Engineered fungus derived FAD-dependent glucose dehydrogenase with acquired ability to utilize hexaammineruthenium (III) as an electron acceptor." *Bioelectrochemistry* 123 (2018): 62-69.

PASSANI, M. B., PANULA, P. LIN, J-S. Histamine in the brain. *Frontiers in systems neuroscience*, 8, 2014, 64.

PERUMAL, V. HASHIM, U. Advances in biosensors: Principle, architecture and applications. *Journal of Applied Biomedicine,* 12.1, 2014, 1-15.

PEELLE, B.R., et al. Design criteria for engineering inorganic material-specific peptides. Langmuir 21,15. (2005), 6929–6933.

PRESNOVA G, et all. Direct heterogeneous electron transfer of recombinant horseradish peroxidases on gold. Faraday Discuss, 116, 2000, 281–289.

REED, T. et al. Crystal structure of histamine dehydrogenase from *Nocardioides simplex. Journal of Biological Chemistry.* 285.33, 2010, 25782-25791.

SARIKAYA, M. Molecular biomimetics: nanotechnology through biology. Nature materials, 2, 2003, 577-585.

SASSOLAS, A.; BLUM, L. J.; LECA-BOUVIER, B. D. Immobilization strategies to develop enzymatic biosensors. Biotechnology advances, 30, 2012, 489-511.

SATO, T.; HORIUCHI, T.; NISHIMURA, I. "Simple and rapid determination of histamine in food using a new histamine dehydrogenase from Rhizobium sp." *Analytical biochemistry* 346.2 (2005): 320-326.

SHAO, Y. et al. Graphene based electrochemical sensors and biosensors: a review. Electroanalysis, 22, 2010, 1027-1036.

SI, B. SONG, E. Recent advances in the detection of neurotransmitters. *Chemosensors* 6.1, 2018, 1.

SIDDIQUI, J. A. et al. Purification and characterization of histamine dehydrogenase from Nocardioides simplex IFO 12069. *FEMS microbiology letters*189.2, 2000, 183-187.

SILVEIRA, C. M.; ALMEIDA, G. "Small electron-transfer proteins as mediators in enzymatic electrochemical biosensors." *Analytical and bioanalytical chemistry* 405.11 (2013): 3619-3635.

SLOCIK JM, WRIGHT DW. Biomimetic mineralization of noble metal nanoclusters. Biomacromolecules 4, 5, 2003. 1135–1141.

SO, C., et al. "Molecular recognition and supramolecular self-assembly of a genetically engineered gold binding peptide on Au {111}." *Acs Nano* 3.6 (2009): 1525-1531.

SO, C.; TAMERLER,C; SARIKAYA, M. "Adsorption, Diffusion, and Self-Assembly of an Engineered Gold-Binding Peptide on Au (111) Investigated by Atomic Force Microscopy." *Angewandte Chemie International Edition* 48.28 (2009): 5174-5177.

TAMERLER, C. et al. Adsorption kinetics of an engineered gold binding peptide by surface plasmon resonance spectroscopy and a quartz crystal microbalance. *Langmuir,* 22.18, 2006, 7712-7718. (a)

TAMERLER, C. et al. Molecular Biomimetics: GEPI Based Biological Routes to Technology. Biopolymers, 94, 2010, 78-94.

THÉVENOT, D. R., et al. Electrochemical biosensors: recommended definitions and classification. *Analytical Letters,* 34.5, 2001, 635-659.

Thurmond, R. ed. *Histamine in inflammation.* Vol. 709. Springer Science & Business Media, 2011.

THURMOND, R. L., GELFAND, E. W., DUNFORD, P. J. The role of histamine H 1 and H4 receptors in allergic inflammation: the search for new antihistamines. *Nature reviews Drug discovery*, 7(1), 2008, 41.

TILIGADA, E. et al. Histamine H3 and H4 receptors as novel drug targets," Expert Opinion on Investigational Drugs, vol.18, no.10, 2009, p.1519–1531.

TSUTSUMI, M. et al. Direct electrochemistry of histamine dehydrogenase from Nocardioides simplex. *Journal of Electroanalytical Chemistry*, 625.2, 2009, 144-148 (b)

TSUTSUMI, M. et al. Site-directed mutation at residues near the catalytic site of histamine dehydrogenase from *Nocardioides simplex* and its effects on substrate inhibition. *Journal of biochemistry,*147.2, 2010, 257-264. (a)

VERMA et al. Enzymatic biosensors for the quantification of biogenic amines: a literature update, Critical Reviews in Biotechnology, 40:1, 2020.

YAMADA, R. et al. Bioelectrochemical determination at histamine dehydrogenase-based electrodes. *Electrochemistry* 76.8, 2008, 600-602.

YANG, C.-C. et al. The primary structure of Hyphomicrobium X dimethylamine dehydrogenase. Eur. J. Biochem. 232, 264–271, 1995.

YANG, M., et al. "Site-specific immobilization of gold binding polypeptide on gold nanoparticle-coated graphene sheet for biosensor application." *Nanoscale* 3.7 (2011): 2950-2956.

YUCESOY, D. T., et al. "Direct bioelectrocatalysis at the interfaces by genetically engineered dehydrogenase." *Bioinspired, Biomimetic and Nanobiomaterials* 4.1 (2015): 79-89.

ZHANG J.K.; CASS A.E.G. A study of his-tagged alkaline phosphatase immobilization on a nanoporous nickel-titanium dioxide film. Anal Biochem 292(2):307–310, 2001

ZHOU, P.; WAGNER, G. "Overcoming the solubility limit with solubility-enhancement tags: successful applications in biomolecular NMR studies." *Journal of biomolecular NMR* 46.1 (2010): 23.